JCI insight

STING activation in alveolar macrophages and group 2 innate lymphoid cells suppresses IL-33-driven type 2 immunopathology

Li She, … , Yong Liu, Xiao-Dong Li

JCI Insight. 2021. https://doi.org/10.1172/jci.insight.143509.

Research In-Press Preview **Immunology** **Inflammation**

2'3'-cGAMP is known as a non-classical 2nd messenger and small immune modulator that possesses potent anti-tumor and antiviral activities through stimulating STING-mediated signaling pathway. However, its function in regulating type 2 immune responses remains unknown. We sought to determine a role of STING activation by 2'3'-cGAMP in type 2 inflammatory reactions in multiple mouse models of eosinophilic asthma. We discovered that 2'3'-cGAMP administration strongly attenuated type 2 lung immunopathology and airway hyperresponsiveness (AHR) induced by IL-33 and a fungal allergen, *A. flavus*. Mechanistically, upon the respiratory delivery, 2'3'-cGAMP was mainly internalized by alveolar macrophages, in which it activated the STING-IRF3-IFN-I signaling axis to induce the production of inhibitory factors containing IFNα, which blocked the IL-33-mediated activation of group 2 innate lymphoid cells (ILC2) in vivo. We further demonstrated that 2'3'-cGAMP directly suppressed the proliferation and function of both human and mouse ILC2 in vitro. Taken together, our findings suggest that STING activation by 2'3'-cGAMP in alveolar macrophages and ILC2 cells can negatively regulate type 2 immune responses, implying that the respiratory delivery of 2'3'-cGAMP might be further developed as an alternative strategy for treating type 2 immunopathologic diseases such as eosinophilic asthma.

STING Activation in Alveolar Macrophages and Group 2 Innate Lymphoid Cells Suppresses IL-33-driven Type 2 Immunopathology

Li She[1,3], Gema D. Barrera[1], Liping Yan[1], Hamad H. Alanazi[1], Edward G. Brooks[2], Peter H. Dube[1], Yilun Sun[1], Hong Zan[1], Daniel P. Chupp[1], Nu Zhang[1], Xin Zhang[3,4,5,6], Yong Liu[3,4,5,6*], Xiao-Dong Li[1*]

[1]Department of Microbiology, Immunology and Molecular Genetics
[2]Division of Immunology and Infectious Disease
Long School of Medicine
University of Texas Health San Antonio

[3]Department of Otolaryngology-Head and Neck Surgery
[4]Clinical Research Center for Pharyngolaryngeal Diseases and Voice Disorders,
[5]Otolaryngology Major Disease Research Key Laboratory of Hunan Province
[6]National Clinical Research Center for Geriatric Disorders
Xiangya Hospital, Central South University

[*]Correspondence: Yong Liu
Department of Otolaryngology-Head and Neck Surgery
Xiangya Hospital, Central South University
87 Xiangya Road, Changsha
Hunan 410008, China

Phone: 86.138.7314.5172
Email: liuyongent@csu.edu.cn

Xiao-Dong Li
Department of Microbiology, Immunology and Molecular Genetics
Long School of Medicine
University of Texas Health Science Center at San Antonio
7703 Floyd Curl Drive-MC 7758
San Antonio, TX 78229-3900

Phone: 1.469.260.9180
Email: lix8@uthscsa.edu

Running Title: **STING activation attenuates type 2 immunopathology**

Conflict of interest: The authors have declared that no conflict of interest exists.

Keywords and Abbreviations

2’3’-cyclic guanosine monophosphate-adenosine monophosphate (2'3'-cGAMP); airway hyperresponsiveness (AHR); alveolar macrophages (AMΦ); *aspergillus flavus* (*A. flavus*); group 2 innate lymphoid cells (ILC2); interferon alpha/beta receptor 1 (IFNAR1); interleukin 33 (IL-33); stimulator of interferon genes (STING); type I interferons (IFN-I);

Abstract

2'3'-cGAMP is known as a non-classical 2nd messenger and small immune modulator that possesses potent anti-tumor and antiviral activities through stimulating STING-mediated signaling pathway. However, its function in regulating type 2 immune responses remains unknown. We sought to determine a role of STING activation by 2'3'-cGAMP in type 2 inflammatory reactions in multiple mouse models of eosinophilic asthma. We discovered that 2'3'-cGAMP administration strongly attenuated type 2 lung immunopathology and airway hyperresponsiveness (AHR) induced by IL-33 and a fungal allergen, *A. flavus*. Mechanistically, upon the respiratory delivery, 2'3'-cGAMP was mainly internalized by alveolar macrophages, in which it activated the STING-IRF3-IFN-I signaling axis to induce the production of inhibitory factors containing IFNα, which blocked the IL-33-mediated activation of group 2 innate lymphoid cells (ILC2) in vivo. We further demonstrated that 2'3'-cGAMP directly suppressed the proliferation and function of both human and mouse ILC2 in vitro. Taken together, our findings suggest that STING activation by 2'3'-cGAMP in alveolar macrophages and ILC2 cells can negatively regulate type 2 immune responses, implying that the respiratory delivery of 2'3'-cGAMP might be further developed as an alternative strategy for treating type 2 immunopathologic diseases such as eosinophilic asthma.

Introduction

Asthma is a chronic condition of airway inflammation characterized by the recurrent episodes of airway obstruction and wheezing. The prevalence and incidence of asthma are very high and still rising in the industrialized world. Clinically, asthma is a very complex and heterogenous disease comprising different subtypes. Eosinophilic asthma is the most common form featured by airway eosinophilia, elevated levels of serum IgE and type 2 cytokines: IL-4, IL-5 and IL-13. Since the primary cause and underlying mechanism of the disease remain poorly understood, current treatments can only provide a long-term control of symptoms, but fail to cure or prevent the disease (1-4).

In the past few years, it has become increasingly appreciated that group 2 innate lymphoid cells (ILC2) play a critical role in the initiation and orchestration of eosinophilic inflammation (5). Innate lymphoid cells lack rearranged antigen receptors expressed on B cells and T cells and are the innate counterparts of T lymphocytes (5-8). By reacting promptly to environmental signals, or type 2 inducer cytokines such as Interleukin 33 (IL-33), activated ILC2s are capable of producing massive amounts of the type 2 cytokines IL-5 and IL-13 (9-12), which promote the development of eosinophilia, airway remodeling and mucus hypersecretion, respectively. Additionally, ILC2-derived IL-13 can potentiate memory T helper 2 cell responses by licensing dendritic cells (13). Notably, IL-33 is a new member of the IL-1 superfamily of cytokines and induces the production of type 2 cytokines in ILC2 and Th2 cells to promote the pathogenesis of many eosinophilic diseases such as asthma (9-12). Due to their enormous capacity in instigating and amplifying type 2 inflammatory responses, activation of ILC2 cells must be tightly regulated. Indeed, emerging evidence suggest that diversified receptors expressed on the surface of ILC2 cells can either enhance or repress their activation and proliferation in response to various signals such as alarmin cytokines, hormones, regulatory cytokines, neuropeptides and lipids (14). Recent studies have also shown that microbial ligands including unmethylated CpG-DNA can activate the corresponding innate immune responses to attenuate eosinophilic inflammation via inhibiting ILC2 function in mouse models of asthma (15-17). However, it is unclear whether other innate immune stimuli such as 2'3'-cGAMP can regulate type 2 immunity through targeting ILC2. 2'3'-cGAMP was discovered as a non-classical 2nd messenger synthesized by the novel DNA sensor cGAS (cyclic GMP-AMP synthase) in response to invasion of cytosolic DNA when mammalian cells are infected by DNA viruses and intracellular bacteria (18-20). 2'3'-cGAMP exclusively binds to and robustly activates STING, which subsequently recruits the kinase TBK1 to trigger a signaling cascade leading to the production of type I interferons (IFN-I). Currently, 2'3'-cGAMP or its derivatives are being intensively investigated in a

number of clinical trials for enhancing the efficacy of anti-PD1-based cancer immunotherapies against multiple tumor types including advanced solid tumors and lymphomas (21-23). In addition, 2'3'-cGAMP can be used as an immune adjuvant to enhance antigen-specific humoral and cellular immunities in a vaccine setting (19).

In this report, we sought to determine an immune modulatory function of 2'3'-cGAMP in regulating type 2 inflammation in multiple mouse models of eosinophilic asthma. We demonstrate that 2'3'-cGAMP triggers the robust production of IFN-I in mouse lungs and strongly suppresses both IL-33 and an environmental allergen *Aspergillus flavus* (*A. flavus*)-induced type 2 lung inflammation and airway hyperreactivity (AHR). Mechanistically, the STING-IFN-I signaling mediates the inhibitory effects of 2'3'-cGAMP and seems to act directly on ILC2 cells to inhibit their proliferation and function in the cytokine production. Collectively, this study identifies an innate immune-driven mechanism for the 2'3'-cGAMP-STING-IFN-I signaling in regulating ILC2 function and demonstrates the potential development of this new mammalian cyclic di-nucleotide for the prevention and treatment of eosinophilic asthma.

Results

2'3'-cGAMP inhibits IL-33-induced type 2 immunopathology. It has been recently shown that 2'3'-cGAMP had a strong immune adjuvant effect to enhance both cellular and humoral immunity (19). However, it remains unexplored whether 2'3'-cGAMP is capable of modulating overzealous type 2 inflammatory responses in the context of eosinophilic asthma. To address this issue, we employed a mouse model of acute lung inflammation induced by a recombinant murine protein IL-33, which is known to robustly activate ILC2-mediated lung inflammation (9, 24). We first determined whether 2'3'-cGAMP could initiate an immune response in mouse lungs. Mice were administered with increasing doses of 2'3'-cGAMP followed by examining lung gene expressions by Real-Time quantitative PCR (RT-qPCR). We found that multiple ISGs (Mx1, ISG15, IFIT3 and OASL2) were strongly induced to reach a peak level of expression by 2'3'-cGAMP at a dose of 5 μg/mouse. Notably, it appears that at this concentration of 2'3'-cGAMP, the induction of two proinflammatory genes IL1β and TNFα were not obvious (Figure 1A). Thus, we chose this dose for the subsequent in vivo experiments in combination with IL-33 (Figure 1B). We found that 2'3'-cGAMP treatment drastically improved IL-33-induced lung pathology characterized by less infiltration of inflammatory cells, reduced epithelial cell hyperplasia and decreased percentage of mucus-producing (PAS+) epithelial cells (Figure 1C). Functionally, 2'3'-cGAMP

treatment resulted in much reduced airway resistance (R) and elastance (E), and increased compliance (C) in response to methacholine (Figure 1D). Consistently, among all analyzed cell types, eosinophils in both bronchoalveolar lavage fluid (BALF) and lungs were dramatically reduced (Figures 1E and 1F, the FACS gating strategy is shown in Figure S1). Notably, the number of neutrophils was also significantly reduced when compared to the IL-33-treated group. Taken together, these results suggest that 2'3'-cGAMP treatment triggered an immune response that strongly inhibits the development of IL-33-driven lung eosinophilia.

2'3'-cGAMP ameliorates lung eosinophilia and AHR induced by a fungal allergen, A. flavus. To evaluate the therapeutic benefit of 2'3'-cGAMP in the context of environmental allergen-driven type 2 lung inflammation, we used a clinically relevant model caused by a fungal allergen *A. flavus* that has been recently shown to act through the IL-33-mediated pathway (25). As with IL-33 above, we challenged mice with 10μg extract of *A. flavus* after exposing mice to 2'3'-cGAMP. We found that *A. flavus*–driven type 2 inflammatory markers were suppressed, as evidenced by the decrease in eosinophil infiltration of BALF and lung in 2'3'-cGAMP-treated mice (Figures 2A and 2B). In addition, the number of neutrophils was also significantly reduced when compared to the *A. flavus*-treated group. 2'3'-cGAMP treatment drastically improved *A. flavus*-induced lung pathology characterized by infiltration of massive inflammatory cells, mucus overproduction (PAS+ epithelial cells) and epithelial cell hyperplasia (Figure 2C). Consistent with these observations, 2'3'-cGAMP treatment improved lung function evidenced by reduced airway resistance, elastance, and improved compliance (Figure 2D). Thus, these data indicate that 2'3'-cGAMP treatment can activate a protective response to attenuate acute type 2 lung inflammation induced by a clinically relevant fungal allergen.

2'3'-cGAMP inhibits ILC2-driven type 2 lung inflammation. Next, we determined whether 2'3'-cGAMP could affect the function and proliferation of lung ILC2 cells in vivo activated by IL-33 or *A. flavus*. In order to easily track the activated population of ILC2 cells, we performed experiments with IL-13 reporter strain (the heterozygous mouse, IL-13-*eGFP*$^{+}$) (26) in addition to wild type mice (Figure 3A). The gating strategy for lung ILC2s is shown in Figure S2. ILC2 expansion was significantly suppressed, as determined by the reduction in total lung ILC2 numbers in both strains of mice in the context of IL-33- or *A. flavus*-treatment. Functionally, the percentage of activated ILC2s (IL-5- and IL-13-double-positive) was also decreased upon treatment of 2'3'-cGAMP (Figures 3B, 3C and 3D). Consistent with previous

experiments, eosinophils in the BALF and lungs were significantly reduced in 2'3'-cGAMP-treated IL-13-*eGFP*$^{+}$ mice (Figures S3). Further, 2'3'-cGAMP-mediated inhibitory effects on the ILC2 proliferation in wild type mice was confirmed by Ki-67 staining (Figure 3E). To further rule out the involvement of adaptive immunity in 2'3'-cGAMP-induced suppressive effects, Rag1$^{-/-}$ mice that lack mature B and T cells were tested in the context of IL-33 or *A. flavus* exposure (Figure 4A). FACS analysis revealed that upon exposures to either IL-33 or *A. flavus*, Rag1$^{-/-}$ mice can develop severe type 2 lung inflammation characterized by the increased eosinophils in both BALF and lungs (Figures 4B and 4C), elevated level of mRNA and protein expressions of type 2 effector cytokines such as IL-5, IL-9 and IL-13 (Figure 4D and 4E), percentages of IL5^{+} & IL13^{+} double positive cells and total numbers of lung ILC2 (Figure S4). Similar to the 2'3'-cGAMP-treated IL-13-*eGFP*$^{+}$ and WT mice, all above examined parameters of type 2 inflammation in Rag1$^{-/-}$ mice were significantly reduced by 2'3'-cGAMP (Figures 4B-4E and S4). Taken together, these results strongly suggest that 2'3'-cGAMP activates an innate immune signaling pathway to negatively regulate ILC2-induced eosinophilic lung inflammation and that suppression is independent of the adaptive immunity in mice.

2'3'-cGAMP inhibits IL-33-, A. flavus- or HDM-induced type 2 inflammation via the STING-IFN-I signaling. Next, we investigated whether the inhibitory effect of 2'3'-cGAMP could be dependent on the STING-IFN-I signaling pathway. As expected, the effect of 2'3'-cGAMP on IL-33-induced type 2 lung inflammation was completely abolished in STING$^{gt/gt}$ mice (Figures 5A, 5B and 5C), indicating the in vivo specificity of 2'3'-cGAMP-activated innate immune responses. As type I interferon responses are known to be a hallmark of the cGAMP-STING signaling (18-20), we then measured the level of IFNα protein in mouse lungs by ELISA. 2'3'-cGAMP treatment, in a dose-dependent manner, triggered a robust production of IFNα protein, which was detected from total lung homogenates (Figure 6A). It is very likely that activation of the 2'3'-cGAMP-STING pathway would generate multiple effector molecules in mouse lungs besides IFN-I. To demonstrate a possible role of IFN-I signaling, we performed a series of experiments using IFNAR1 deficient mice. The expression of a stimulatory molecule CD40 in bone marrow-derived DCs (BM-DC) and alveolar macrophages derived from IFNAR1$^{-/-}$ mice were greatly reduced when stimulated with 2'3'-cGAMP (Figure 6B). More importantly, in contrast to wild type mice shown in Figures 1 and 2, IFNAR1$^{-/-}$ mice treated with either IL-33 or IL-33+2'3'-cGAMP did not show any significant differences in eosinophils and ILC2 (number and percentage) in BALF or lungs (Figures 6C, 6D and 6E). We also explored the possibility whether the eosinophilia and activation of ILC2 cells

could be inhibited by 2'3'-cGAMP co- or post-delivered with *A. flavus* in Rag1$^{-/-}$ mice (Figure S5) or WT mice (Figure S6). In addition, we examined whether 2'3'-cGAMP treatment can affect the established type 2 lung inflammation induced by house dust mite extract (HDM), a more physiologically relevant aeroallergen (Figure S7A). As shown in Figure S7B-D, 2'3'-cGAMP treatment significantly inhibited HDM-induced lung eosinophilia and activation of ILC2 cells. In all these treatments, 2'3'-cGAMP was effective in suppressing type 2 immunopathology. Taken together, these results suggest that the STING-IFN-I signaling axis mediates the effector function of 2'3'-cGAMP in vivo to negatively regulate type 2 lung inflammation induced by IL-33 and natural allergens likely via suppressing the activation of ILC2 cells.

Activation of alveolar macrophages by 2'3'-cGAMP leads to the production of ILC2 inhibitory factors. To identify lung cell types that are responsible for taking up 2'3'-cGAMP, we performed a flow cytometric analysis of lung cells (FACS gating strategy, Figure 7A). Mice were treated with fluorescently labeled 2'3'-cGAMP (cGAMP-Fluo) and lungs were collected post 16 hours. Lung tissues were then digested and cells were stained with various cell type specific surface makers. Interestingly, cGAMP-Fluo was mainly detected in alveolar macrophages, and to a lesser extent, monocyte-derived DC (MoDC), but not other examined lung immune cells such as cDCs, interstitial-MΦ, monocytes, T cells, B cells, and non-immune cells (CD45- cells) (Figure 7B). FACS analysis further revealed that the phosphorylated form of IRF3 in alveolar macrophages appeared within 1-2 hours after the 2'3'-cGAMP treatment (Figure 7C). STING is indispensable for the in vivo activity of 2'3'-cGAMP because the phosphorylated form of IRF3 was only detected in the lung homogenates of wild type, but not in STING$^{gt/gt}$ mice (Figure 7D). To determine whether 2'3'-cGAMP-stimulated AMΦ could produce interferons or ILC2 regulatory factors, we collected conditional media from the cultured AMΦ as illustrated in Figure 8A. As expected, IFNα was only detected in the conditional media (CM) of AMΦ from WT, but not STING deficient mice by ELISA (Figure 8B). Moreover, while it had no effects on the non-activated ILC2 cells under the conditions of media or IL-2 + IL-7, the conditional media from 2'3'-cGAMP-treated WT-AMΦ significantly impaired the growth and function of IL-33-activated ILC2 cells measured by the cell number and proliferation marker Ki-67 (Figures 8C, 8D and 8E) and the cytokine levels of IL-5 and IL-13 (Figure 8F). To further demonstrate an important role of AMΦ in mediating the effects of 2'3'-cGAMP in vivo, we have performed IL-33 treatments in two mouse lines lacking AMΦ (Figures S8A and S9A), Csf2$^{-/-}$ and clodronate liposome-treated WT mice, in which type 2 inflammatory

responses were poorly activated (Figures S8 and S9). Nonetheless, it appears that the 2'3'-cGAMP administration could further reduce the numbers of eosinophils and ILC2 when compared to the mouse lines lacking AMΦ treated with the IL-33 alone, implying that 2'3'-cGAMP might act on other cell types such as ILC2 in vivo. Overall, these results indicate that alveolar macrophages have the ability to take up extracellular 2'3'-cGAMP and turns on the STING-IRF3 pathway that may lead to the production of ILC2 inhibitory factors such as type I interferons.

2'3'-cGAMP directly suppresses the proliferation and cytokine production of human and mouse ILC2 in vitro. Because we have shown above that 2'3'-cGAMP treatment could act on alveolar macrophages to negatively regulate ILC2-driven type 2 inflammation, next we wanted to assess its potential effect on ILC2 cells in vitro. The purified mouse and human ILC2 cells (Figure S10) were cultured under conditions of media alone, IL-2 + IL-7, or IL-2 + IL-7 plus IL-33 and stimulated with 2’3’-cGAMP. Indeed, the purified mouse and human ILC2 cells were able to take up 2’3’-cGAMP and activate the STING-IFN-I pathway (Figure S11). Further, in a concentration-dependent manner, 2’3’-cGAMP strongly suppressed the proliferation of both mouse and human ILC2 cells demonstrated by the cell density, the cell number and the level of Ki-67 (Figures 9A, 9B and 9C, 10A and 10B). We found that this suppression by 2’3’-cGAMP was partly due to the induction of cell death (Figure 9D). Moreover, 2’3’-cGAMP strongly suppressed the production of IL-5 and IL-13 by mouse and human ILC2 cells activated by IL-33 (Figures 9E and 10C). Intracellular cytokine staining also demonstrated that 2’3’-cGAMP also suppressed the cytokine expression inside the ILC2 cells (Figures 9F and 10D). Moreover, 2’3’-cGAMP at a lower concentration (5 μg/ml), when compared to two other TLR agonists (R848, a TLR7 agonist and CpG-A, a TLR9 agonist), appears to be more potent in directly suppressing both the growth and production of type 2 effector cytokines of human ILC2 cells (Figures 10E and 10F). Notably, at a higher concentration (25 μg/ml), all three agents had inhibitory effects on human ILC2. Collectively, these results indicate that 2’3’-cGAMP can directly suppress the activation of ILC2 function induced by IL-33. Taken all together, our data indicate that type I interferon signaling mediates the effector function of 2'3'-cGAMP to negatively regulate allergen-induced type 2 immune responses. Based on these findings, as depicted in Figure 11, we propose a working model for 2'3'-cGAMP in modulating ILC2-mediated type 2 immunity. After the respiratory delivery, 2'3'-cGAMP is first taken up by alveolar macrophages where it activates the STING-mediated pathway to induce the production of type I interferons, which may in turn act on ILC2 cells to restrain their abilities to proliferate and produce type

2 cytokines. In addition, 2'3'-cGAMP seems to be able to directly suppress the function of activated ILC2 cells in the context of exposure to IL-33 and environmental allergens such as *A. flavus*.

Discussion

In this study, we reveal an important role for 2'3'-cGAMP in negatively regulating type 2 inflammation induced by IL-33, a fungal allergen and HDM. We demonstrate that 2'3'-cGAMP administration efficiently protects mice from both IL-33- and a fungal allergen-induced AHR. Mechanistically, 2'3'-cGAMP can directly act on both alveolar macrophages and ILC2 cells. In alveolar macrophages, 2'3'-cGAMP activates the STING-IRF3 pathway that leads to a rapid production of ILC2 suppressive factors such as IFNα. These data provide proof-of-concept evidence to support a therapeutic value of 2'3'-cGAMP in preventing and mitigating lung inflammation of eosinophilic asthma.

A few recent studies have shown that type I interferons directly inhibit the function and proliferation of ILC2 in vitro and in vivo during influenza A infection or treatment with TLRs agonists such as CpG-DNA and R848 (15, 16, 27-30). Interestingly, our results suggest that the inhibitory effects of 2'3'-cGAMP are likely to be attributed, at least in part, to its ability in triggering production of interferons in mouse lungs, which generates a Th1-dominant cytokine milieu that is suppressive to ILC2 cells, which may further lead to a reduced level of Th2-biased adaptive immune response. In a recent Phase II clinical trial, administering inhaled recombinant IFNα/β (rIFN) was effective in treating steroid-resistant eosinophilic asthma (31). However, an interferon-based therapy is often associated with a wide array of adverse effects (32, 33). Therefore, instead of using cytokines directly, agonists that specifically stimulate the innate immune system are becoming more favorable therapeutics largely due to their lower toxicity and better immune response profile. In this regard, our study presents an important proof-of-principle for treating eosinophilic asthma through harnessing 2'3'-cGAMP-STING-mediated innate immune response.

Due to its inherent dual negative charges and the presence of an extracellular enzyme such as ecto-nucleotide pyrophosphatase/phosphodiesterase (ENPP1) (34), an efficient in vivo delivery of 2'3'-cGAMP was usually considered to be very challenging without proper formulations. However, our results show that when administered intratracheally at a low dose, 2'3'-cGAMP was capable of inducing innate immune responses comprising type I interferons that were sufficient to inhibit ILC2 activation by IL-33 or a fungal allergen, *A flavus*. Given that alveolar macrophages (AMΦ) are the first line of phagocytic defense in lower airways and are approximately 50 times more numerous than cDCs, it was not

unexpected that 2'3'-cGAMP was found to be mainly taken up by AMΦ, to a lesser extent, MoDCs in mouse lungs. It is possible that the 2'3'-cGAMP-activated AMΦ can produce chemokines and cytokines including type I interferons to create a suppressive local environment against the development of overzealous type 2 inflammation upon exposures to various aeroallergens. In the context of allergic inflammation, inflamed lung tissue may become leaky and allow immune cell or cytokines to travel or penetrate across tissue barriers to act on ILC2 cells. However, the molecular mechanism of how 2'3'-cGAMP enters the cytosol of AMΦ where it engages the downstream STING-IFN-I signaling pathway remains unknown. In this regard, two recent reports suggest that two proteins, cGAS and human SLC19A1 might be involved in trafficking of extracellular 2'3'-cGAMP into the cytoplasm of cultured macrophages and monocytes (35, 36). Additionally, in contrast to bacterial cyclic di-nucleotides (3'3'-c-di-GMP, 3'3'-c-di-AMP and 3'3'-cGAMP), which preferentially bind with high affinity and activate two new sensors ERAdP (37) and RECON (37-40), 2′3′cGAMP is a much more potent and specific ligand for human STING (41, 42). Collectively, it appears that 2′3′-cGAMP would be a promising candidate for harnessing innate immunity to treat or prevent many human diseases such as cancer and eosinophilic asthma.

At present, a number of STING agonists have entered clinical trials for cancer immunotherapy (21-23). It can also be envisioned that many issues or concerns such as adverse effects may arise and must be further addressed with independent experimental approaches. At the same time, there will be more exciting opportunities on the parallel development of these reagents for other applications such as treating eosinophilic diseases. Supported by this work, the use of 2’3-cGAMP or other STING agonists as immune modulators to enhance the efficacy of allergen immunotherapy (AIT) merits future investigation.

To some extent, our current findings on 2’3-cGAMP are consistent with a new report showing that a bacterial cyclic di-nucleotide, c-di-GMP can effectively inhibit IL-33- or *Alternaria*-induced type 2 inflammation in mice (43). However, it has also recently been reported that in another model of allergic inflammation, the administration of 2'3'-cGAMP had an adjuvant effect that exacerbated the HDM-induced Th2 response (44). This result is contrast to our data presented in Figure S7, in which HDM-induced type 2 inflammation was attenuated by 2'3'-cGAMP administration. The exact causes for these discrepancies are unclear and could be ascribed to many things such as the dose, timing, delivery route for 2′3′-cGAMP. More preclinical experiments are needed in order to resolve this controversy.

In conclusion, our results highlight the role of an allergen-independent, innate immune-driven effector function triggered by the 2'3'-cGAMP-STING-IFN-I signaling pathway, which robustly counteracts the rapidly activated ILC2s in the context of IL-33 and a fungal allergen-induced acute type 2 inflammation. From the therapeutic standpoint, our study suggests that further development of a formulated 2'3'-cGAMP for local delivery into the lungs may serve as an alternative approach for preventing or treating eosinophilic asthma.

Methods

Mice. IL-13-*eGFP* reporter strain (26) and STING$^{gt/gt}$ (45) mice have been described previously. Wild type C57BL/6J, Csf2$^{-/-}$, IFNAR1$^{-/-}$ and Rag1$^{-/-}$ mice were purchased from the Jackson Laboratory. The IL-13-*eGFP*$^{+}$ heterozygous mice were generated by intercrossing with wild type C57BL/6J on campus. Mice were bred and maintained under specific pathogen-free conditions in the animal facility. Age-matched (8-10 weeks old) female mice were used for the experiments.

Cells and reagents. Bone marrow cells were collected from femurs and tibiae of mice. To obtain BM-DC, about 10 million bone marrow cells were cultured in DMEM containing 10% FCS, antibiotics and Flt3 ligand. After 7 days, mature DCs were harvested and cultured in 96-well plates for experiments. Media was changed every other day. 2'3'-cGAMP was purchased from InvivoGen.

ELISA to detect cytokines in mouse lungs and cell culture supernatants. For measuring cytokines in mouse lungs after 2'3'-cGAMP stimulation, the harvested lungs were washed once with cold PBS, transferred into 2 mL tubes, rapidly frozen into liquid-N2 and stored at −80°C. Later, to prepare lung homogenates, 1 mL tissue protein extraction reagent (T-PER) (Thermo) containing protease inhibitors (Roche) was added and homogenized by a BeadBeater (BioSpec). The lysates were transferred to a 1.5 mL tube and spun at 14,000×g for 30 min at 4°C. Supernatant was collected for the ELISA measurement of cytokines. IFNα in supernatant of alveolar macrophages culture and lung homogenates were measured with the ELISA kit (PBL Assay Science). Cytokines such as TNFα, IL-5, IL-9, IL-13 and IFNγ in lung homogenates and type 2 cytokines (IL-5 and IL-13) in supernatants of mouse or human ILC2 cell cultures were analyzed with ELISA kit (all purchased from Invitrogen), IL1β in lung homogenates was detected by the ELISA kit (R&D systems). All final reactions were developed with TMB substrate (Thermo scientific) and stopped by sulfuric acid (0.16M), and the OD at 450 nm was measured.

Western Blot. Western Blotting was performed as previously described with some modifications (46). Briefly, protein extracts were obtained from the lungs of 8-wk-old female mice treated with 2'3'-cGAMP (5 μg/mouse) for different time periods. Half of lung tissue was put into lysing Matrix D tube (MP Biomedicals) and immediately frozen in liquid N2. 1.0 mL of Extraction Buffer (8M urea, 1% SDS, 0.15M Tris-HCl pH 7.5) was added and samples were homogenized by a BeadBeater (BioSpec). The lysates were transferred to a 1.5 mL tube and spun at 14,000×g for 30 min at 4°C. Supernatant was collected and protein concentration was measured by Bradford protein assay (Pierce^{TM}). 55 μg of each sample was loaded and separated in 10% SDS/PAGE and transferred to PVDF (Millipore). Membranes

were blocked with 5% nonfat milk and incubated with rabbit monoclonal antibodies against IRF3, P-IRF3 and β-actin (Cell Signaling).

Real-Time Quantitative PCR. Reverse transcription and real-time PCR (qPCR) reactions were carried out using iScript cDNA synthesis kit and iQ SYBR Green Supermix (Bio-Rad). qPCR was performed on a Bio-Rad CFX384 Touch™ Real-Time PCR Detection System using the following primers: Mouse Primers, Forward (5'→3'); Reverse (5'→3'): Rpl19 (AAATCGCCAATGCCAACTC; TCTTCCCTATGCCCATATGC), IL1β (TCTATACCTGTCCTGTGTAATG; GCTTGTGCTCTGCTTGTG), IFIT3 (TGGCCTACATAAAGCACCTAGATGG; CGCAAACTTTTGGCAAACTTGTCT), ISG15 (GAGCTAGAGCCTGCAGCAAT; TTCTGGGCAATCTGCTTCTT), Mx1 (TCTGAGGAGAGCCAGACGAT; ACTCTGGTCCCCAATGACAG), OASL2 (GGATGCCTGGGAGAGAATCG; TCGCCTGCTCTTCGAAACTG), TNFα (CCTCCCTCTCATCAGTTCTATGG; GGCTACAGGCTTGTCACTCG), IL-5 (AGGATGCTTCTGCACTTGAG; CCTCATCGTCTCATTGCTTG), IL-9 (GAACATCACGTGTCCGTCCT; CGGCTTTTCTGCCTTTGCAT), IL-13 (TGAGCAACATCACACAAGACC; AGGCCATGCAATATCCTCTG).

In vivo administration and FACS analysis of BALF and lung. Mice were anesthetized by isofluorane inhalation, followed the 3 times of intra-tracheal administration with 2'3'-cGAMP (5 μg), rIL-33 (0.25 μg), or *A. flavus* protease allergen (10 μg) in 80 μl of PBS as shown Figure 1B. Mice were sacrificed at indicated times and the trachea was catheterized and flushed with 1 mL of ice-cold PBS-EDTA three times. Differential cells in BALF were labeled with antibodies as indicated, then mixed with counting beads (Spherotech) for further FACS analysis on a BD Celesta cell analyzer. Flow cytometry data were analyzed using FlowJo software. The antibodies and reagents for FACS analysis are listed below: SPHERO™ AccuCount Fluorescent (Spherotech, Cat.# ACFP-70-5), Anti-Mouse Siglec-F PE (clone E50-2440) (BD Bioscience, Cat.# 552126), Anti-Mouse CD19 Alexa Fluor® 647 (clone 1D3) (BD Bioscience, Cat.# 557684), Anti-Mouse CD3ε APC (clone 145-2C11) (BioLegend, Cat.# 100322), Anti-Mouse MHC II APC-Cy7 (clone M5/114.15.2) (BioLegend, Cat.# 10627), Anti-Mouse CD11c PE-Cy7 (clone N418) (TONBO bioscience, Cat.# 60-0114-U100), Anti-Mouse CD11b V450 Rat (clone M1/70) (BD Bioscience, Cat.# 560456), Anti-Mouse Ly-6G FITC (clone RB6-8C5) (Invitrogen, Cat.# 11-5931-82), Anti-Mouse Fixable Viability Dye eFluor 506 (Invitrogen, Cat.# 65-0866-14), Anti-Mouse CD45 PerCP-Cy5.5 (clone: 30-F11) (BioLegend, Cat.# 103130), Anti-Mouse CD45 APC-Cy7 (clone

30-F11) (BD Bioscience, Cat.# 561037), Anti-Mouse CD103 Alexa Fluor®647 (clone: 2ET) (BioLegend, Cat.# 121410), Anti-Mouse CD64 PE (clone X54-5/7.1) (BioLegend, Cat.# 139303), Anti-Mouse Ly6C PerCP-Cy5.5 (clone: AL-21) (BD Bioscience, Cat.# 560525), Anti-Mouse Siglec-F FITC (clone S17007L) (BioLegend, Cat.# 155503), Anti-Mouse CD64 FITC (clone X54-5/7.1) (BioLegend, Cat.# 139316), Anti-Mouse CD40 PE (clone 3/23) (BioLegend, Cat.# 124609), Anti-Mouse Isotype Ctrl PE (clone RTK2071) (BioLegend, Cat.# 400408), Anti-Mouse P-IRF3 (S396) Alexa Fluor®488 (clone: D601M) (Cell Signaling, Cat.# 53539S), Anti-Mouse Isotype Ctrl FITC (clone RTK2758) (BioLegend, Cat.# 400506).

Identification of lung ILC2. Lung ILC2 identification was performed as described previously (47). Lung tissues were digested in 8 mL RPMI-1640 containing Liberase (50 μg/mL) and DNase I (1 μg/mL) for about 40 min at 37 °C. Cell suspensions were filtered through 70 μm cell strainers and washed once with RPMI-1640. For ILC2 identification, total lung cell suspensions were blocked with 2.4G2 antibodies and stained with lineage cocktail mAbs (CD3ε, CD4, CD8α, CD11c, FceRIα, NK1.1, CD19, TER119, CD5, F4/80, Gr-1, and Ly6G), PE-conjugated T1/ST2, PerCP-Cy5.5-conjugated CD25, V450-conjugated Sca-1, PE-Cy7-conjugated KLRG1, APC-Cy7-conjugated CD45 and eFluor 506 Fixable Viability Dye.

Intranuclear and intracellular staining. Intranuclear staining of Ki-67 and transcription factors was performed with the True-Nuclear™ Transcription Factor Buffer Set (BioLegend) according to the manufacturer's instructions. For intracellular cytokine staining, single-cell suspensions from the lungs of mice were prepared with Liberase™ (50 μg/mL) and DNase I (1 μg/mL). 2 x 10^6 total live nucleated cells were stimulated in 200 μL RPMI-1640 media containing 10% FBS, Penicillin/Streptomycin (P+S), 2-mercaptoethanol (2-ME, 50 μM), brefeldin A (GolgiPlug™, BD Biosciences) and PMA (phorbol 12-myristate 13-acetate) (30 ng/mL) at 37 °C for 3 hours. After surface staining, cells were fixed and permeabilized with BioLegend Cytofix/Perm buffer and further stained intracellularly with anti-mouse IL-5 and IL-13. Dead cells were stained with eFluor506 Fixable Viability Dye before fixation and permeabilization and excluded during analysis.

ILC2 cell sorting and culture. Murine Lung ILC2s were isolated from $Rag1^{-/-}$ mice treated with IL-33 (0.25 μg/mouse) for three consecutive days plus 2 days of resting before processing lung tissues for sorting ILC2 cells with an BD FACSAria cell sorter. The criteria for identifying ILC2 is lacking classical lineage markers (CD3ε, CD4, CD8α, CD11c, FceRIα, NK1.1, CD19, TER119, CD5, F4/80 and Gr-1), but expressing markers of CD45 and T1/ST2. The purity of sorted ILC2s should be greater than

95%. Sorted ILC2s were cultured and expanded in PRMI 1640 media supplemented with 10% FBS, murine IL-2 and IL-7 (all at 10 ng/mL) in 96-well round plates for 6 days before further experiments.

Human ILC2s were isolated from peripheral blood of healthy donors or umbilical cord blood samples from healthy full-term births in the Department of Obstetrics and Gynecology of UT Health San Antonio. All human samples were used in compliance with UT Health San Antonio Institutional Review Board. Peripheral or Cord Blood Mononuclear Cells (PBMCs or CBMCs) were isolated from diluted umbilical cord blood (1:2) by density gradient centrifugation using density gradient medium, Histopaque® (Sigma Aldrich) and SepMate^{TM} 50 mL tubes (STEMCELL Technologies) (47, 48). Cells were then washed once with dPBS-FBS buffer (dPBS, 3% fetal bovine serum, 1mM EDTA) and resuspended in dPBS-FBS. Cells were stained with antibodies against CD45 and lineage markers (CD3, CD14, CD16, CD19, CD20 and CD56), and ILC2 markers CRTH2, CD127 and CD45. Human ILC2s were sorted by the BD FACSAria cell sorter as $CD45^{+}Lin^{-}CRTH2^{+}CD127^{+}$ cells. The purity of sorted ILC2s was determined to be greater than 95%. Sorted human ILC2s were cultured and expanded in PRMI 1640 media supplemented with 10% FBS, rh-IL-2 and rh-IL-7 (all at 50 ng/mL) in 96-well round plates for 6 days before further experiments.

Culture and treatment of mouse and human ILC2 cells. Sorted ILC2 were cultured with or without 2'3'-cGAMP (5 μg/mL and 25 μg/mL) in 200 μL complete PRMI 1640 media with or without murine IL-2, IL-7 and IL-33 (all at 10ng/mL) in 96-well round plates (2000 cells/well) in a 37℃ incubator with 5% CO_2. 3 days later, the percentage of $IL\text{-}5^{+}IL13^{+}$ cells, expression of Ki-67 and apoptosis of ILC2 cells were analyzed by flow cytometry. 5 days later, the number and proliferation of ILC2 cells were analyzed by flow cytometry, and the supernatant were collected for further detecting of IL-5 and IL-13 by ELISA.

Sorted human ILC2 were cultured in the complete PRMI 1640 media (200 μL) with or without rh-IL-2, rh-IL-7 and rh-IL-33 (all at 50 ng/mL) in 96-well round plates (2,000 cells/well) in a 37℃ incubator with 5% CO_2. The cells were treated with 2'3'-cGAMP, R848 and CpG-A (5 or 25 μg/mL as indicated) for 3 or 5 days. The percentage of $IL\text{-}5^{+}IL13^{+}$ cells, the expression of Ki-67 of ILC2 cells were analyzed on day 3 by flow cytometry. On day 5, the number and proliferation of ILC2 cells were analyzed by flow cytometry, and the levels of IL-5 and IL-13 in the supernatants were measured by ELISA.

Culture and treatment of murine alveolar macrophages. Murine alveolar macrophages were obtained from bronchoalveolar lavage fluids (BALFs) of WT and $STING^{gt/gt}$ mice. Briefly, BALFs were centrifuged at 1,500g for 7 minutes. Freshly isolated cells were resuspended in complete media (RPMI 1640, 10% FCS, 1% penicillin-streptomycin) with GM-CSF (10 ng/mL, PEProtech) in 96-well round

plates (10, 000 cells/well) in a 37℃ incubator with 5% CO_2. After 24h, the nonadherent cells were discarded, the plates were washed with warm PBS and cultured in fresh complete media with GM-CSF (10 ng/mL). 6 days later, these alveolar macrophages from WT and $STING^{gt/gt}$ mice were treated with or without 2'3'-cGAMP (25 μg/mL) in 200 μL complete PRMI 1640 media for another 3 days. Then, the supernatants were collected for further treating murine ILC2 cells and detection of mouse IFNα production by ELISA.

Depletion of alveolar macrophages using clodronate liposomes. To deplete lung macrophages, mice were intra-tracheally administered once with 80 μL of a clodronate-loaded liposome suspension (Liposoma BV). Control mice were injected with 80 μL PBS-loaded liposomes. To evaluate the efficacy and kinetics of the depletion by clodronate-loaded liposomes, the number of alveolar macrophages in BAFL and lung was determined by FACS as shown in Figure S9A.

Lung inflammation and pathology. Each mouse was intra-tracheally administered IL-33 or *A. flavus* with or without 2'3'-cGAMP. Two days after the last challenge lung tissues were taken and fixed in 4% paraformaldehyde, paraffin embedded, cut into 4-μm sections, and stained with hematoxylin and eosin (H&E) and periodic acid-Schiff (PAS). Complete images of control and treated lungs were obtained digitally using the Aperio Scanscope XT (Aperio, Vista, CA). Magnification ×200 was used for scoring the percentage of PAS+ (mucus-producing) bronchial epithelial cells. At least five fields were scored to obtain the average for each mouse as previously described (49-51).

Measurement of pulmonary function. In the IL-33- and *A. flavus*-induced lung inflammation model, changes in mouse pulmonary function after allergen exposure were determined by invasive measurements using the Flexivent system (Scireq, Montreal, PQ, Canada). On day 5, the trachea was intubated after anesthetization. The lungs were mechanically ventilated. Indicators of airway hyperreactivity (AHR), including airway resistance (R), elastance (E) and compliance (C), were measured after increasing doses (6.25–50 mg/mL) of aerosolized methacholine.

Statistics. The statistical analysis was done using software GraphPad Prism 6. For comparison of two groups, P values were determined by unpaired two-tailed Student's t test, unless otherwise indicated. For comparison of more than two groups, Two-Way ANOVA was performed. P value<0.05 was considered statistically significant. P values are indicated on plots and in figure legends. P value $\geqslant 0.05$ was not considered statistically significant [N.S.], * $p < 0.05$, ** $p < 0.01$, *** $p < 0.001$, **** $p < 0.0001$.

Study approval. All experiments were performed by following the experimental protocols approved by the Institutional Animal Care and Use Committee (IACUC) of University of Texas Health Science Center at San Antonio.

Author contributions

L.S., G.D.B., L.Y., H.H.A. and Y.S. performed most experiments; L.S., G.D.B., L.Y., H.H.A. E.G.B., P.H.D., Y.S., H.Z., D.P.C., N.Z., X.Z., Y.L. and X.-D.L. analyzed data; L.S., G.D.B., L.Y., H.H.A., Y.L. and X.-D.L. planned, designed research. L.S., Y.L. and X.-D.L. wrote the manuscript; All authors discussed the results and participated in writing and commenting on the manuscript.

Acknowledgements

We thank Dr. Na Xiong for critical reading of the manuscript and Ms. Karla Gorena for technical assistance in flow cytometry. L.S. is supported by the China Scholarship Council and Hunan Provincial Innovation Foundation for Postgraduate (CX201713068). H.H.A. is supported by the Department of Clinical Laboratory Sciences, College of Applied Medical Sciences, Jouf University, Sakaka, Saudi Arabia. X.-D.L. is supported by the UT Health San Antonio School of Medicine Startup Fund and the Max and Minnei Voelcker Fund.

REFERENCES AND NOTES

1. Eder W, Ege MJ, and von Mutius E. The asthma epidemic. *N Engl J Med.* 2006;355(21):2226-35.
2. Hamid Q, and Tulic M. Immunobiology of asthma. *Annu Rev Physiol.* 2009;71:489-507.
3. Lambrecht BN, and Hammad H. The immunology of the allergy epidemic and the hygiene hypothesis. *Nat Immunol.* 2017;18(10):1076-83.
4. Holgate ST, Wenzel S, Postma DS, Weiss ST, Renz H, and Sly PD. Asthma. *Nat Rev Dis Primers.* 2015;1:15025.
5. Vivier E, Artis D, Colonna M, Diefenbach A, Di Santo JP, Eberl G, et al. Innate Lymphoid Cells: 10 Years On. *Cell.* 2018;174(5):1054-66.
6. Eberl G, Colonna M, Di Santo JP, and McKenzie AN. Innate lymphoid cells. Innate lymphoid cells: a new paradigm in immunology. *Science.* 2015;348(6237):aaa6566.
7. Artis D, and Spits H. The biology of innate lymphoid cells. *Nature.* 2015;517(7534):293-301.
8. Barlow JL, and McKenzie ANJ. Innate Lymphoid Cells of the Lung. *Annu Rev Physiol.* 2019;81:429-52.
9. Liew FY, Girard JP, and Turnquist HR. Interleukin-33 in health and disease. *Nat Rev Immunol.* 2016;16(11):676-89.
10. Cayrol C, and Girard JP. Interleukin-33 (IL-33): A nuclear cytokine from the IL-1 family. *Immunol Rev.* 2018;281(1):154-68.
11. Kubo M. Innate and adaptive type 2 immunity in lung allergic inflammation. *Immunol Rev.* 2017;278(1):162-72.
12. Molofsky AB, Savage AK, and Locksley RM. Interleukin-33 in Tissue Homeostasis, Injury, and Inflammation. *Immunity.* 2015;42(6):1005-19.
13. Halim TY, Hwang YY, Scanlon ST, Zaghouani H, Garbi N, Fallon PG, et al. Group 2 innate lymphoid cells license dendritic cells to potentiate memory TH2 cell responses. *Nat Immunol.* 2016;17(1):57-64.
14. Hurrell BP, Shafiei Jahani P, and Akbari O. Social Networking of Group Two Innate Lymphoid Cells in Allergy and Asthma. *Front Immunol.* 2018;9:2694.
15. Thio CL, Lai AC, Chi PY, Webster G, and Chang YJ. Toll-like receptor 9-dependent interferon production prevents group 2 innate lymphoid cell-driven airway hyperreactivity. *J Allergy Clin Immunol.* 2019.
16. Maazi H, Banie H, Aleman Muench GR, Patel N, Wang B, Sankaranarayanan I, et al. Activated plasmacytoid dendritic cells regulate type 2 innate lymphoid cell-mediated airway hyperreactivity. *J Allergy Clin Immunol.* 2018;141(3):893-905 e6.
17. Sabatel C, Radermecker C, Fievez L, Paulissen G, Chakarov S, Fernandes C, et al. Exposure to Bacterial CpG DNA Protects from Airway Allergic Inflammation by Expanding Regulatory Lung Interstitial Macrophages. *Immunity.* 2017;46(3):457-73.
18. Sun L, Wu J, Du F, Chen X, and Chen ZJ. Cyclic GMP-AMP synthase is a cytosolic DNA sensor that activates the type I interferon pathway. *Science.* 2013;339(6121):786-91.
19. Li XD, Wu J, Gao D, Wang H, Sun L, and Chen ZJ. Pivotal roles of cGAS-cGAMP signaling in antiviral defense and immune adjuvant effects. *Science.* 2013;341(6152):1390-4.
20. Wu J, Sun L, Chen X, Du F, Shi H, Chen C, et al. Cyclic GMP-AMP is an endogenous second messenger in innate immune signaling by cytosolic DNA. *Science.* 2013;339(6121):826-30.
21. Corrales L, McWhirter SM, Dubensky TW, Jr., and Gajewski TF. The host STING pathway at the interface of cancer and immunity. *J Clin Invest.* 2016;126(7):2404-11.
22. Corrales L, Glickman LH, McWhirter SM, Kanne DB, Sivick KE, Katibah GE, et al. Direct Activation of STING in the Tumor Microenvironment Leads to Potent and Systemic Tumor Regression and Immunity. *Cell Rep.* 2015;11(7):1018-30.
23. Ng KW, Marshall EA, Bell JC, and Lam WL. cGAS-STING and Cancer: Dichotomous Roles in Tumor Immunity and Development. *Trends Immunol.* 2018;39(1):44-54.
24. Schmitz J, Owyang A, Oldham E, Song Y, Murphy E, McClanahan TK, et al. IL-33, an interleukin-1-like cytokine that signals via the IL-1 receptor-related protein ST2 and induces T helper type 2-associated cytokines. *Immunity.* 2005;23(5):479-90.
25. Cayrol C, Duval A, Schmitt P, Roga S, Camus M, Stella A, et al. Environmental allergens induce allergic inflammation through proteolytic maturation of IL-33. *Nat Immunol.* 2018;19(4):375-85.
26. Neill DR, Wong SH, Bellosi A, Flynn RJ, Daly M, Langford TK, et al. Nuocytes represent a new innate effector leukocyte that mediates type-2 immunity. *Nature.* 2010;464(7293):1367-70.
27. Duerr CU, McCarthy CD, Mindt BC, Rubio M, Meli AP, Pothlichet J, et al. Type I interferon restricts type 2 immunopathology through the regulation of group 2 innate lymphoid cells. *Nat Immunol.* 2016;17(1):65-75.
28. Moro K, Kabata H, Tanabe M, Koga S, Takeno N, Mochizuki M, et al. Interferon and IL-27 antagonize the function of group 2 innate lymphoid cells and type 2 innate immune responses. *Nat Immunol.* 2016;17(1):76-86.

Figure 1

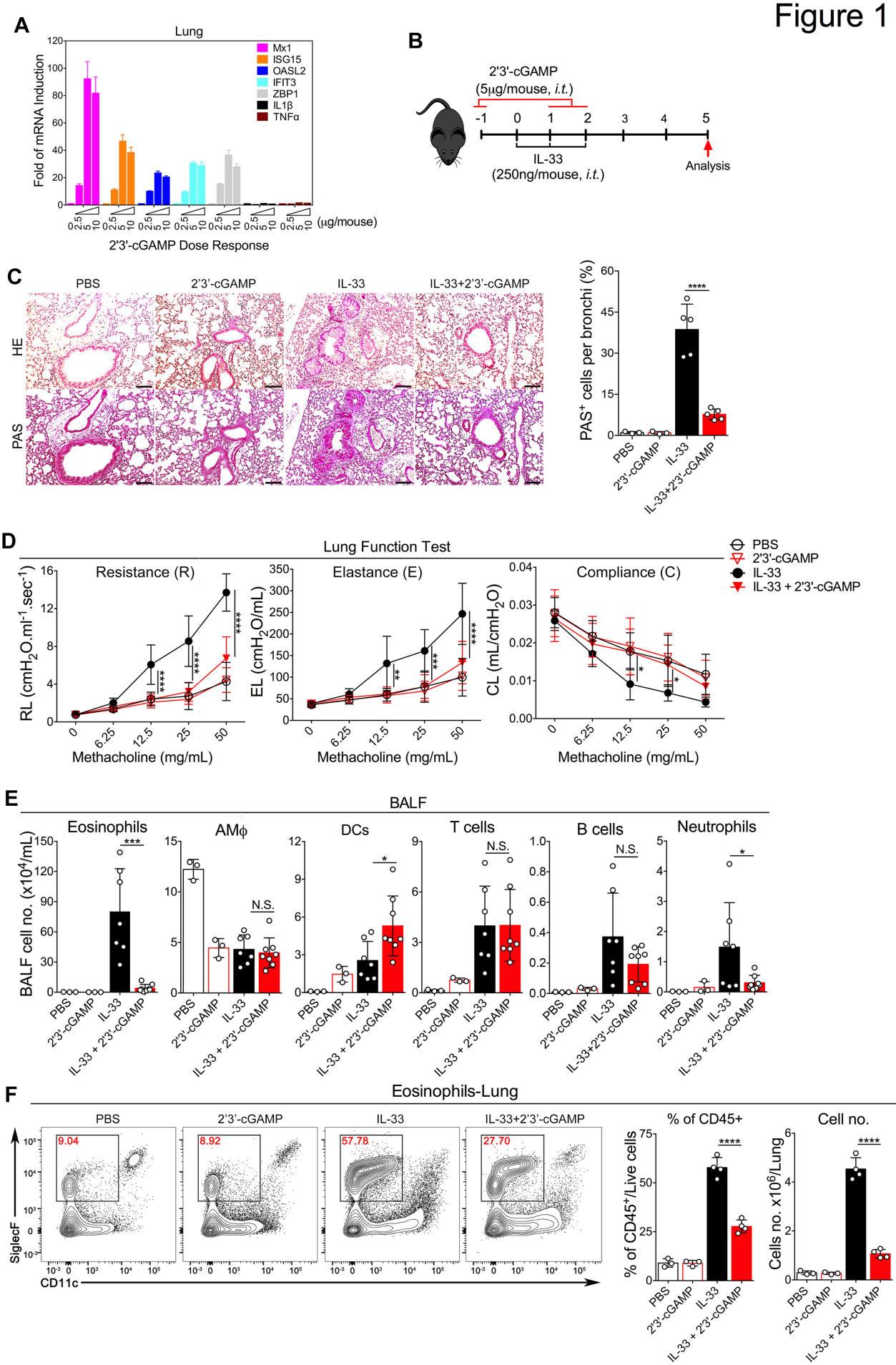
A
Lung
Mx1
ISG15
OASL2
IFIT3
ZBP1
IL1β
TNFα
Fold of mRNA Induction
(μg/mouse)
2'3'-cGAMP Dose Response
B
2'3'-cGAMP
(5μg/mouse, i.t.)
IL-33
(250ng/mouse, i.t.)
Analysis
C
PBS
2'3'-cGAMP
IL-33
IL-33+2'3'-cGAMP
HE
PAS
PAS+ cells per bronchi (%)
D
Lung Function Test
Resistance (R)
Elastance (E)
Compliance (C)
Methacholine (mg/mL)
PBS
2'3'-cGAMP
IL-33
IL-33 + 2'3'-cGAMP
E
BALF
Eosinophils
AMϕ
DCs
T cells
B cells
Neutrophils
BALF cell no. (x10⁴/mL)
N.S.
F
Eosinophils-Lung
SiglecF
CD11c
% of CD45+
Cell no.
% of CD45+/Live cells
Cells no. x10⁶/Lung

Figure 1. 2'3'-cGAMP inhibits IL-33-induced type 2 lung inflammation. (**A**) Transcriptional induction of mouse lung gene expressions by 2'3'-cGAMP. Error bars represent standard error of triplicate assays. Representative data from one experiment are shown here. Similar results were obtained from at least three experiments. (**B**) Experimental setup illustrating the animal groups, the regimen and timeline. (**C**) Lung pathologies were assessed with H&E and PAS staining. Representative images (scale bars, 100 μm) and the percentage of PAS+ cells are shown here. Magnification ×200 was used for counting the percentage of mucus-producing bronchial epithelial cells-(PAS+). (**D**) Lung functions were examined by Flexivent (Scireq). Airway resistance (R), elastance (E) and compliance (C) were measured after exposure to increasing doses (6.25-50 mg/mL) of aerosolized methacholine. (n=4-6, P value <0.05 was considered statistically significant, 2way ANOVA, Tukey's multiple comparisons test, * $p < 0.05$, ** $p < 0.01$, *** $p < 0.001$, **** $p < 0.0001$). (**E**) Groups of mice as indicated were treated with PBS, 2'3'-cGAMP, IL-33 or IL-33+2'3'-cGAMP**.** Bronchoalveolar lavage fluid (BALF) was collected and analyzed for differential immune cell types. The result was a pool of two independent experiments. (n=3-8 per group as indicated with open circles, P value <0.05 was considered statistically significant, unpaired t-test, * $p < 0.05$, *** $p < 0.001$). (**F**) Administration of 2'3'-cGAMP decreased the percentage and number of lung eosinophils after exposure to IL-33. (n=3-4 per group as indicated with open circles, P value <0.05 was considered statistically significant, unpaired t-test, **** $p < 0.0001$).

Figure 2

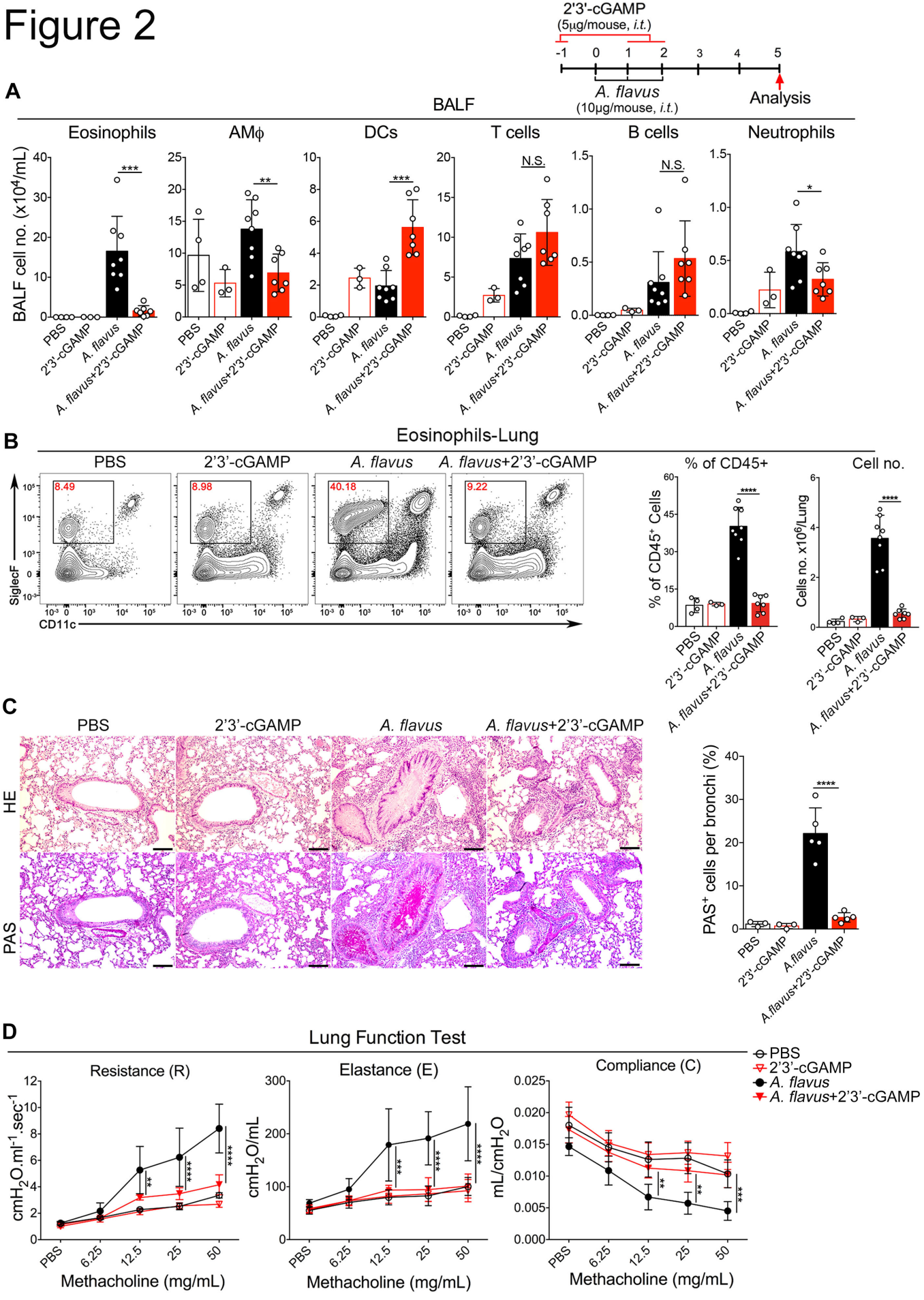
2'3'-cGAMP
(5μg/mouse, i.t.)
-1
0
1
2
3
4
5
A. flavus
(10μg/mouse, i.t.)
Analysis
A
BALF
Eosinophils
AMϕ
DCs
T cells
B cells
Neutrophils
BALF cell no. (x10⁴/mL)
N.S.
PBS
2'3'-cGAMP
A. flavus
A. flavus+2'3'-cGAMP
B
Eosinophils-Lung
PBS
2'3'-cGAMP
A. flavus
A. flavus+2'3'-cGAMP
8.49
8.98
40.18
9.22
SiglecF
CD11c
% of CD45+
Cell no.
% of CD45⁺ Cells
Cells no. x10⁶/Lung
C
HE
PAS
PAS⁺ cells per bronchi (%)
D
Lung Function Test
Resistance (R)
Elastance (E)
Compliance (C)
cmH2O.ml-1.sec-1
cmH2O/mL
mL/cmH2O
Methacholine (mg/mL)

Figure 2. 2'3'-cGAMP inhibits *A. flavus*-induced type 2 lung inflammation. (**A**) Groups of mice as indicated were treated with PBS, 2'3'-cGAMP, *A. flavus* or *A. flavus*+2'3'-cGAMP. BALF was collected and analyzed for differential immune cell types. The result was a pool of two independent experiments. (n=3-7 per group as indicated with open circles, P value <0.05 was considered statistically significant, unpaired t-test, * $p < 0.05$, ** $p < 0.01$, *** $p < 0.001$). (**B**) Administration of 2'3'-cGAMP decreased the percentage and number of lung eosinophils after exposure to *A. flavus*. (n=3-8 per group as indicated with open circles, P value <0.05 was considered statistically significant, unpaired t-test, **** $p < 0.0001$). (**C**) Lung pathologies were assessed with H&E and PAS staining. Representative images (scale bars, 100 μm) and the percentage of PAS+ cells are shown here. Magnification ×200 was used for counting the percentage of mucus-producing bronchial epithelial cells-(PAS+). (**D**) Airway hyperreactivity (AHR) was examined by Flexivent (Scireq). Airway resistance (R) was measured after exposure to increasing doses (6.25-50 mg/mL) of aerosolized methacholine. (n=3-5 per group as indicated with open circles, P value <0.05 was considered statistically significant, 2way ANOVA, Tukey's multiple comparisons test, ** $p < 0.01$, *** $p < 0.001$, **** $p < 0.0001$).

Figure 3

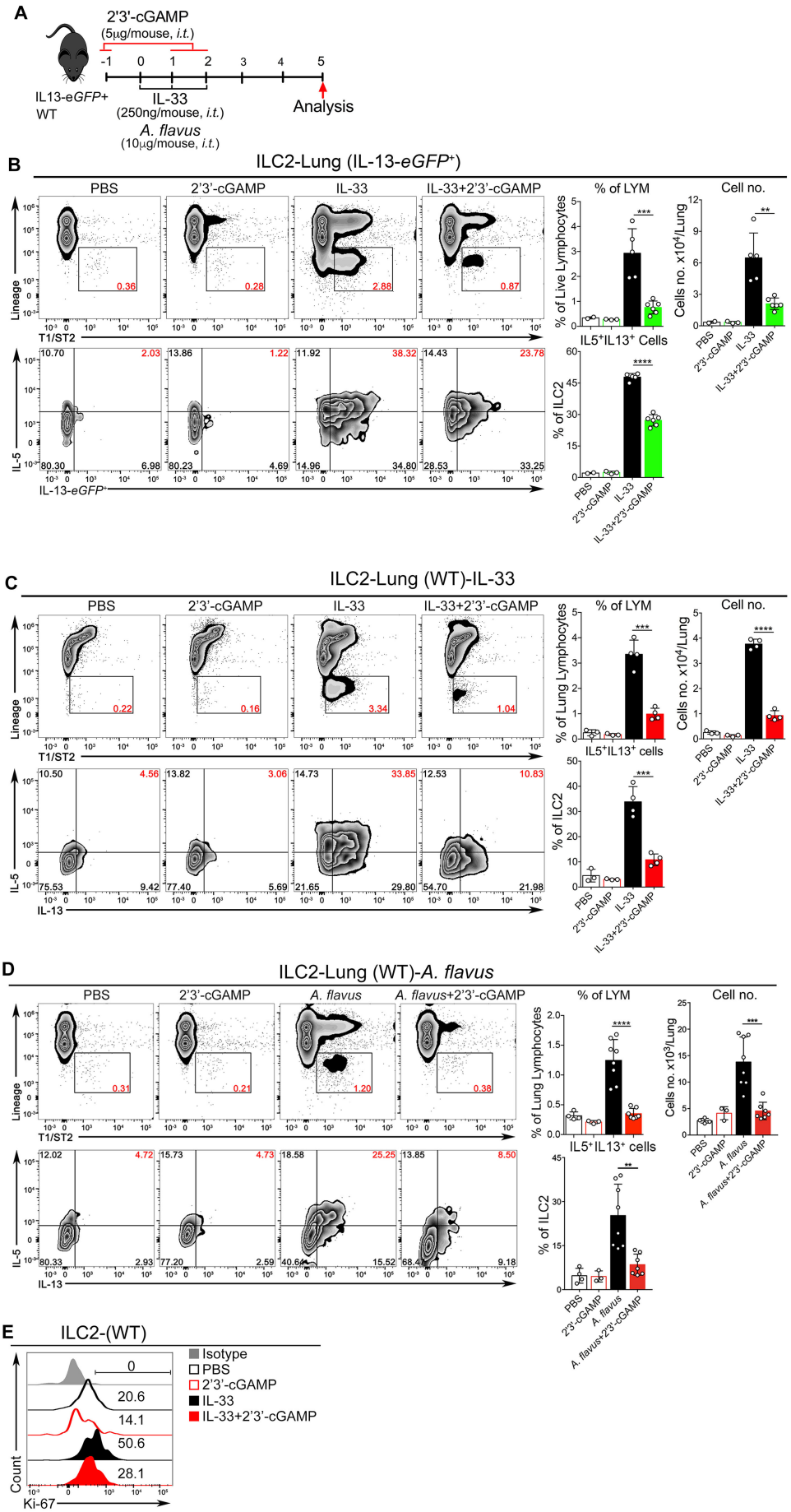
A
2'3'-cGAMP
(5μg/mouse, i.t.)
-1 0 1 2 3 4 5
IL13-eGFP+
WT
IL-33
(250ng/mouse, i.t.)
A. flavus
(10μg/mouse, i.t.)
Analysis
B
ILC2-Lung (IL-13-eGFP+)
PBS
2'3'-cGAMP
IL-33
IL-33+2'3'-cGAMP
Lineage
T1/ST2
IL-5
IL-13-eGFP+
0.36
0.28
2.88
0.87
10.70
2.03
13.86
1.22
11.92
38.32
14.43
23.78
80.30
6.98
80.23
4.69
14.96
34.80
28.53
33.25
% of LYM
% of Live Lymphocytes
Cell no.
Cells no. x10⁴/Lung
IL5+IL13+ Cells
% of ILC2
C
ILC2-Lung (WT)-IL-33
0.22
0.16
3.34
1.04
10.50
4.56
13.82
3.06
14.73
33.85
12.53
10.83
75.53
9.42
77.40
5.69
21.65
29.80
54.70
21.98
IL-13
% of Lung Lymphocytes
D
ILC2-Lung (WT)-A. flavus
A. flavus
A. flavus+2'3'-cGAMP
0.31
0.21
1.20
0.38
12.02
4.72
15.73
4.73
18.58
25.25
13.85
8.50
80.33
2.93
77.20
2.59
40.64
15.52
68.47
9.18
Cells no. x10³/Lung
E
ILC2-(WT)
Count
Ki-67
0
20.6
14.1
50.6
28.1
Isotype
PBS
2'3'-cGAMP
IL-33
IL-33+2'3'-cGAMP

Figure 3. 2'3'-cGAMP inhibits ILC2 activation and proliferation induced by IL-33 and *A. flavus* in WT or IL-13 reporter mice. (**A**) Experimental protocol showing the animal groups (IL-13-*eGFP*$^{+}$ and WT), the corresponding treatment regimen and timeline. (**B**) The heterozygous IL-13-*eGFP*$^{+}$ mice were treated with PBS, 2'3'-cGAMP, IL-33 or IL-33+2'3'-cGAMP. Lung single cell suspensions were prepared and the number of ILC2 cells in lungs were analyzed. In addition, lung cells were stimulated with PMA in cultures as described in the Methods. The percentage of IL5^{+}IL13^{+}-double positive ILC2 cells in lungs were analyzed. (n=2-6 per group as indicated with open circles). (**C**) Similar to (**B**), instead, WT mice were used. (n=3-4 per group as indicated with open circles). (**D**) Similar to (**C**), instead of IL-33, WT mice were treated with *A. flavus*. (n=3-8 per group as indicated with open circles). For (**A**), (**B**) and (**C**), P value <0.05 was considered statistically significant, unpaired t-test, ** $p < 0.01$, *** $p < 0.001$, **** $p < 0.0001$. (**E**) WT mice were treated with PBS, 2'3'-cGAMP, IL-33 or IL-33+2'3'-cGAMP. The lung ILC2 cells were analyzed with Ki-67 staining and isotype antibody. The result is a representative of two independent experiments.

Figure 4

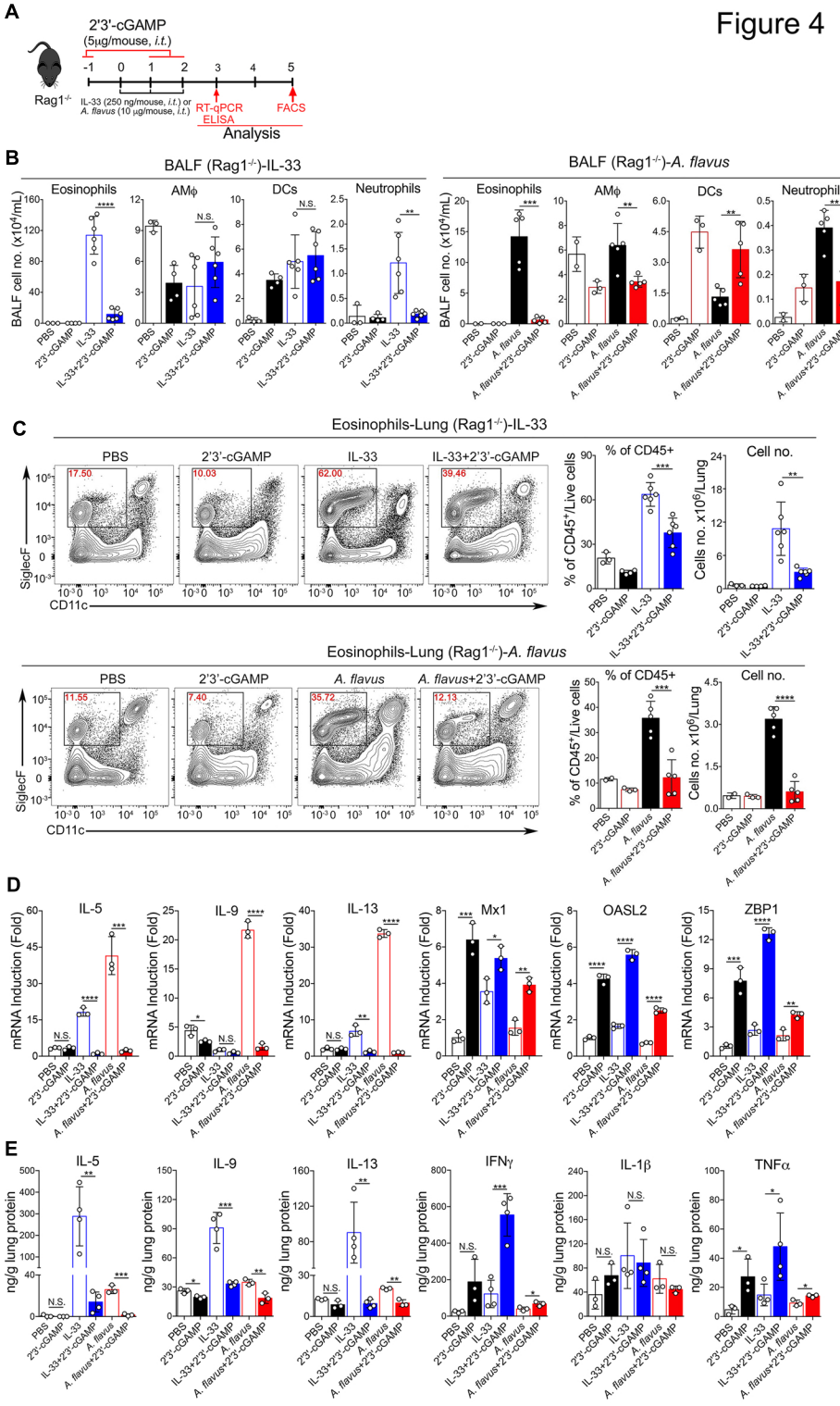
A
2'3'-cGAMP
(5μg/mouse, i.t.)
-1 0 1 2 3 4 5
Rag1-/-
IL-33 (250 ng/mouse, i.t.) or
A. flavus (10 μg/mouse, i.t.)
RT-qPCR
ELISA
FACS
Analysis
B
BALF (Rag1-/-)-IL-33
BALF (Rag1-/-)-A. flavus
Eosinophils
AMφ
DCs
Neutrophils
BALF cell no. (x10⁴/mL)
PBS
2'3'-cGAMP
IL-33
IL-33+2'3'-cGAMP
A. flavus
A. flavus+2'3'-cGAMP
N.S.
C
Eosinophils-Lung (Rag1-/-)-IL-33
Eosinophils-Lung (Rag1-/-)-A. flavus
SiglecF
CD11c
% of CD45+
% of CD45+/Live cells
Cell no.
Cells no. x10⁶/Lung
D
IL-5
IL-9
IL-13
Mx1
OASL2
ZBP1
mRNA Induction (Fold)
E
IFNγ
IL-1β
TNFα
ng/g lung protein

Figure 4. 2'3'-cGAMP inhibits type 2 lung inflammation induced by IL-33 and *A. flavus* in Rag1$^{-/-}$ mice. (**A**) Experimental protocol showing the animal groups of Rag1$^{-/-}$ mice and the corresponding treatment regimen and timeline. (**B**) Administration of 2'3'-cGAMP into Rag1$^{-/-}$ mice decreased the number of airway eosinophils. BALF analysis of Rag1$^{-/-}$ mice were treated with two kinds of experimental regimens, PBS, 2'3'-cGAMP, IL-33, IL-33+2'3'-cGAMP (left panel) or PBS, 2'3'-cGAMP, *A. flavus*, *A. flavus*+2'3'-cGAMP (right panel). (**C**) Similar to (**B**), administration of 2'3'-cGAMP into Rag1$^{-/-}$ mice decreased the percentage and number of lung eosinophils after exposure to IL-33 (upper panel) or *A. flavus* (lower panel). (n=2-5 per group as indicated with open circles, P value <0.05 was considered statistically significant, unpaired t-test, ** $p < 0.01$, *** $p < 0.001$, **** $p < 0.0001$). (**D**) Similar to (**B**), instead, lung samples were collected on day 3 for RNA extraction, then RT-qPCR analysis of the selected type 2 effector cytokines and ISGs as indicated were performed. Error bars represent standard error of triplicate assays. Representative data from one experiment are shown here. Similar results were obtained from at least three experiments. (**E**) Similar to (**B**), instead, lung samples were collected and homogenized on day 3 for protein extractions, which were used for measuring the level of the selected cytokine as indicated by ELISA. For (**D**) and (**E**), n=3-4 per group as indicated with open circles, P value <0.05 was considered statistically significant, unpaired t-test, * $p < 0.05$, ** $p < 0.01$, *** $p < 0.001$).

Figure 5

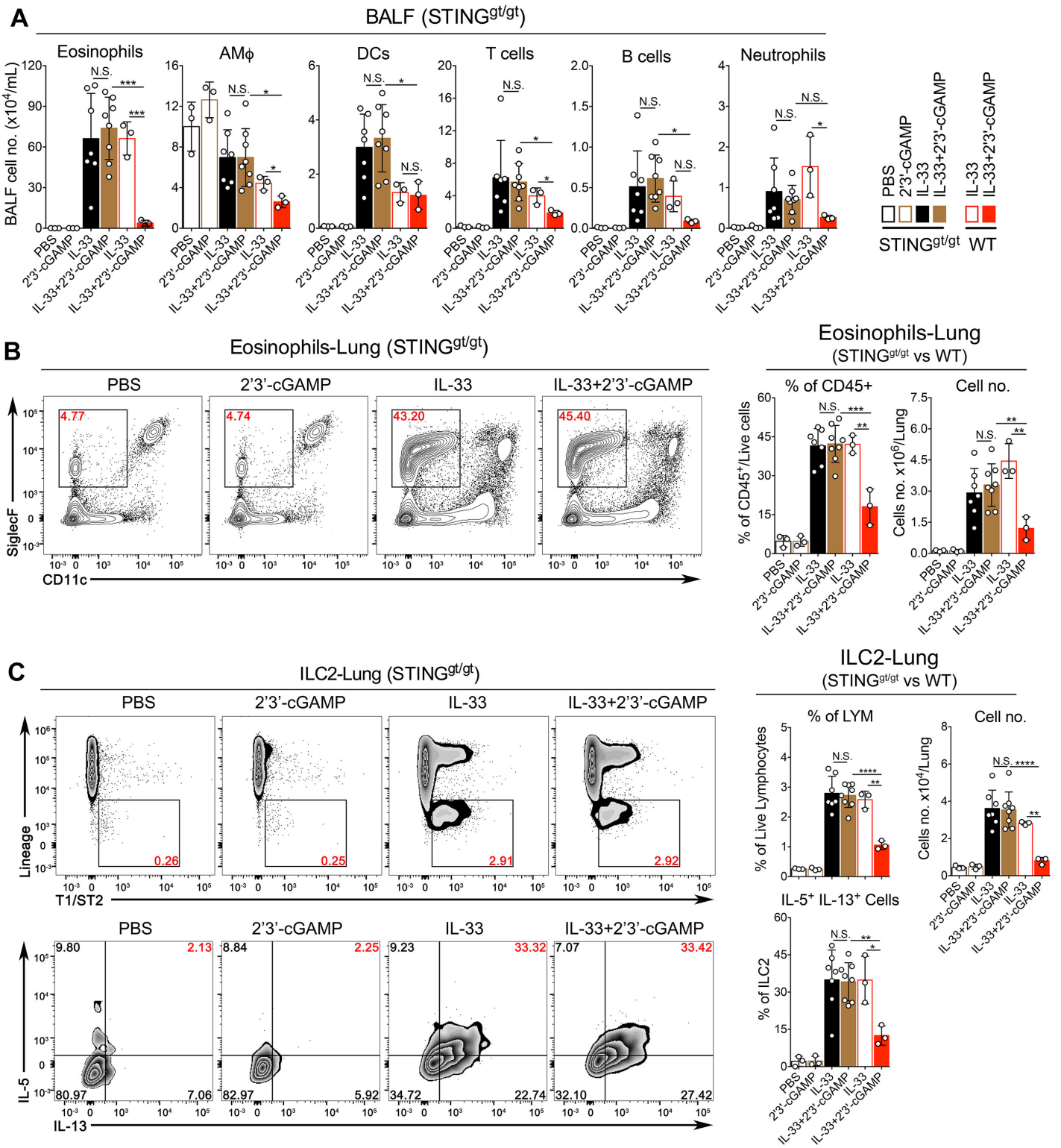
A
BALF (STINGgt/gt)
Eosinophils
AMϕ
DCs
T cells
B cells
Neutrophils
BALF cell no. (x10⁴/mL)
N.S.
PBS
2'3'-cGAMP
IL-33
IL-33+2'3'-cGAMP
STINGgt/gt
WT
B
Eosinophils-Lung (STINGgt/gt)
PBS
2'3'-cGAMP
IL-33
IL-33+2'3'-cGAMP
4.77
4.74
43.20
45.40
SiglecF
CD11c
Eosinophils-Lung
(STINGgt/gt vs WT)
% of CD45+
% of CD45+/Live cells
Cell no.
Cells no. x10⁶/Lung
C
ILC2-Lung (STINGgt/gt)
Lineage
T1/ST2
0.26
0.25
2.91
2.92
IL-5
IL-13
9.80
2.13
80.97
7.06
8.84
2.25
82.97
5.92
9.23
33.32
34.72
22.74
7.07
33.42
32.10
27.42
ILC2-Lung
(STINGgt/gt vs WT)
% of LYM
% of Live Lymphocytes
Cell no.
Cells no. x10⁴/Lung
IL-5⁺ IL-13⁺ Cells
% of ILC2

Figure 5. The inhibitory effect of 2'3'-cGAMP is abolished in STING-deficient mice. Groups of $STING^{gt/gt}$ and WT mice were treated with PBS, 2'3'-cGAMP, IL-33 or IL-33+2'3'-cGAMP as indicated. BALF was collected and analyzed for differential immune cell types. (**A**) In contrast to WT mice, administration of 2'3'-cGAMP into $STING^{gt/gt}$ mice did not significantly change number of airway eosinophils after exposure to IL-33. (**B**) Similar to (**A**), administration of 2'3'-cGAMP in $STING^{gt/gt}$ mice did not significantly change the percentage and number of lung eosinophils after exposure to IL-33. (**C**) Similar to (**A**), the number and percentage of $IL5^{+}IL13^{+}$-double positive ILC2 cells in lungs of $STING^{gt/gt}$ mice were analyzed. (n=3-5 per group as indicated with open circles, P value ≥0.05 was not considered statistically significant [N.S.], unpaired t-test, * $p < 0.05$, ** $p < 0.01$, *** $p < 0.001$, **** $p < 0.0001$).

Figure 6

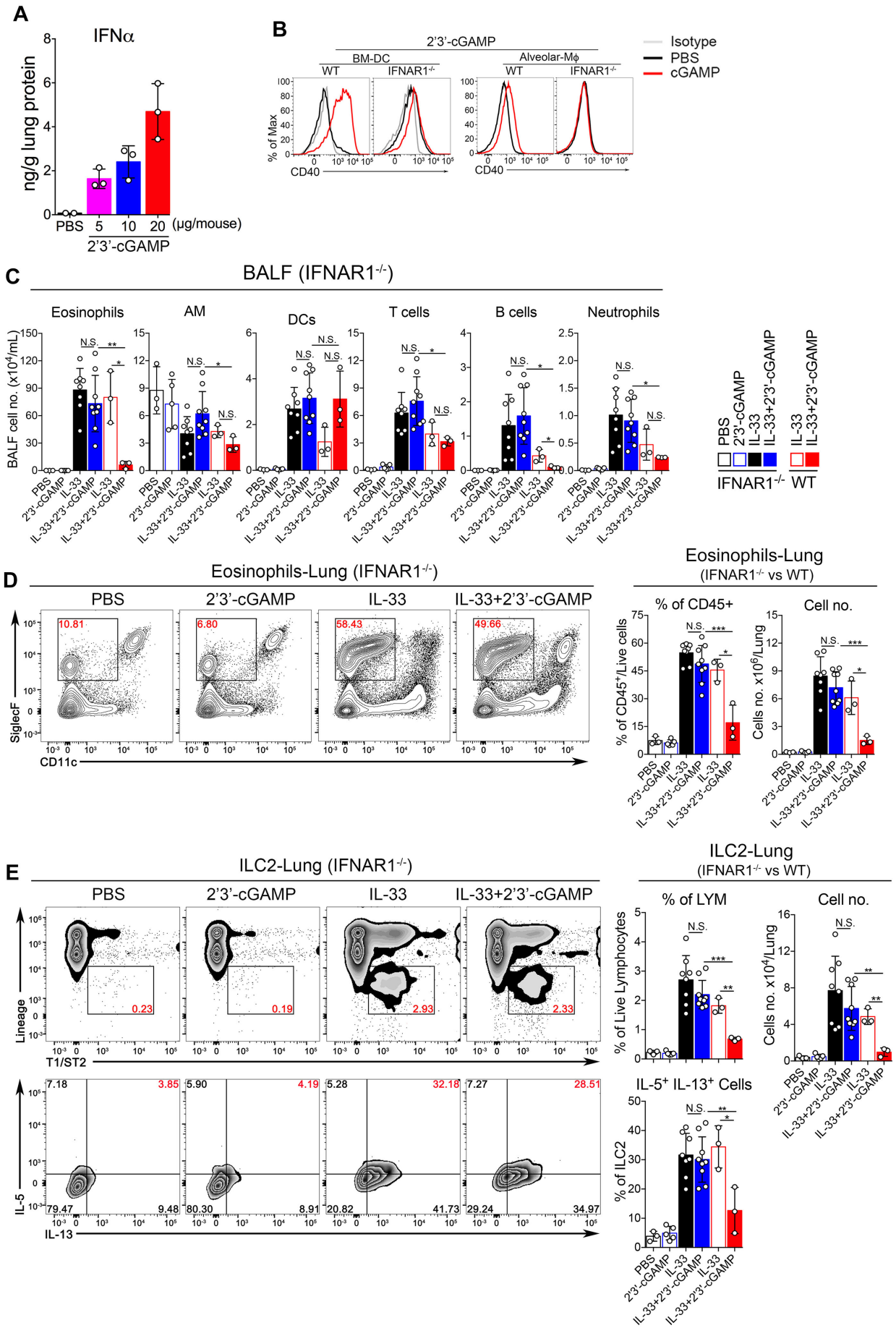
A
IFNα
ng/g lung protein
PBS
5
10
20
(μg/mouse)
2'3'-cGAMP
B
2'3'-cGAMP
BM-DC
Alveolar-Mϕ
WT
IFNAR1-/-
Isotype
PBS
cGAMP
% of Max
CD40
C
BALF (IFNAR1-/-)
Eosinophils
AM
DCs
T cells
B cells
Neutrophils
BALF cell no. (x10^4/mL)
N.S.
PBS
2'3'-cGAMP
IL-33
IL-33+2'3'-cGAMP
IFNAR1-/-
WT
D
Eosinophils-Lung (IFNAR1-/-)
PBS
2'3'-cGAMP
IL-33
IL-33+2'3'-cGAMP
10.81
6.80
58.43
49.66
SiglecF
CD11c
Eosinophils-Lung
(IFNAR1-/- vs WT)
% of CD45+
Cell no.
% of CD45+/Live cells
Cells no. x10^6/Lung
E
ILC2-Lung (IFNAR1-/-)
0.23
0.19
2.93
2.33
Lineage
T1/ST2
7.18
3.85
79.47
9.48
5.90
4.19
80.30
8.91
5.28
32.18
20.82
41.73
7.27
28.51
29.24
34.97
IL-5
IL-13
ILC2-Lung
(IFNAR1-/- vs WT)
% of LYM
Cell no.
% of Live Lymphocytes
Cells no. x10^4/Lung
IL-5+ IL-13+ Cells
% of ILC2

Figure 6. The inhibitory effect of 2'3'-cGAMP is mediated by the IFN-I signaling pathway. (**A**) The induction of IFNα protein after administration of 2'3'-cGAMP at 5, 10 and 20 μg/mouse for 24 hours. The mouse lungs from wild type mice were processed for the ELISA measurement. (**B**) BM-DC and alveolar macrophages derived from WT and IFNAR1$^{-/-}$ mice were treated with 2'3'-cGAMP. Then, the expression of a co-stimulatory molecule CD40 was analyzed by FACS. (**C**) Groups of IFNAR1$^{-/-}$ and WT mice were treated with PBS, 2'3'-cGAMP, IL-33 or IL-33+2'3'-cGAMP as indicated. BALF was collected and analyzed for differential immune cell types. In contrast to WT mice, administration of 2'3'-cGAMP into IFNAR1$^{-/-}$ mice did not significantly change number of airway eosinophils after exposure to IL-33. (**D**) Administration of 2'3'-cGAMP in IFNAR1$^{-/-}$ mice did not significantly decrease the percentage and number of lung eosinophils after exposure to IL-33. (**E**) Similar to (**C**), the number and percentage of IL5^{+}IL13^{+}-double positive ILC2 cells in lungs of IFNAR1$^{-/-}$ mice were analyzed. (n=3-7 per group as indicated with open circles, P value ≥0.05 was not considered statistically significant [N.S.], unpaired t-test, * $p < 0.05$, ** $p < 0.01$, *** $p < 0.001$).

Figure 7

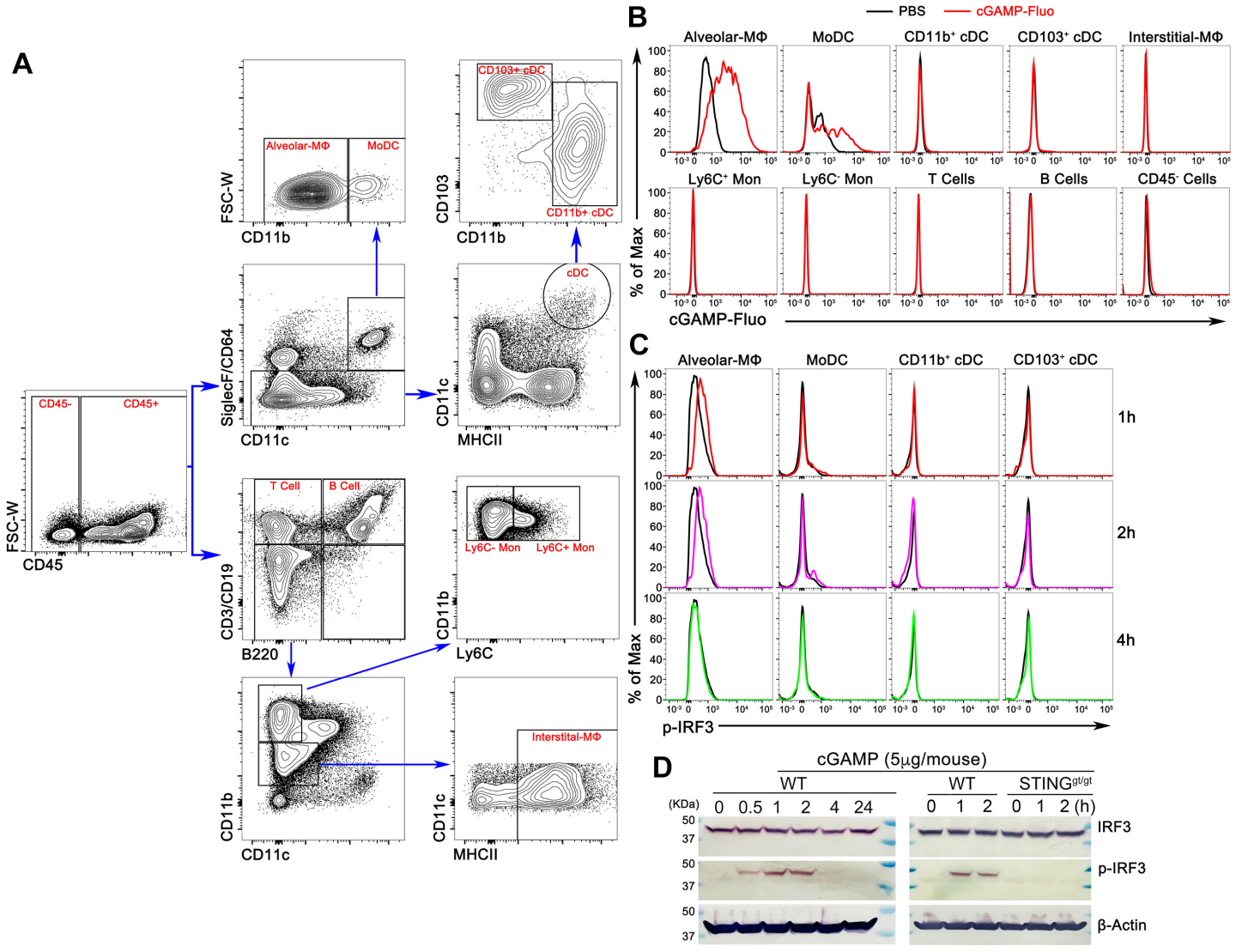

Figure 7. 2'3'-cGAMP is mainly taken up by alveolar macrophages in vivo. (**A**) FACS gating strategy for identification of specific lung cell types by staining cell surface markers as indicated in the Materials and Methods. (**B**) The fluorescence-labelled 2'3'-cGAMP was mainly detected by FACS analysis in alveolar macrophages, to a lesser extent, monocyte-derived DC (MoDC), but not in other lung cell types. The result is a representative of three independent experiments. (**C**) FACS analysis shows that the phosphorylated form of IRF3 can be detected in alveolar macrophages at 1-2 hours post the 2'3'-cGAMP treatment. The result is a representative of three independent experiments. (**D**) Western Blot analysis of homogenates of mouse lungs shows that 2'3'-cGAMP treatment rapidly activates the STING-mediated pathway within 1-2 hours that results in the phosphorylation of IRF3.

Figure 8

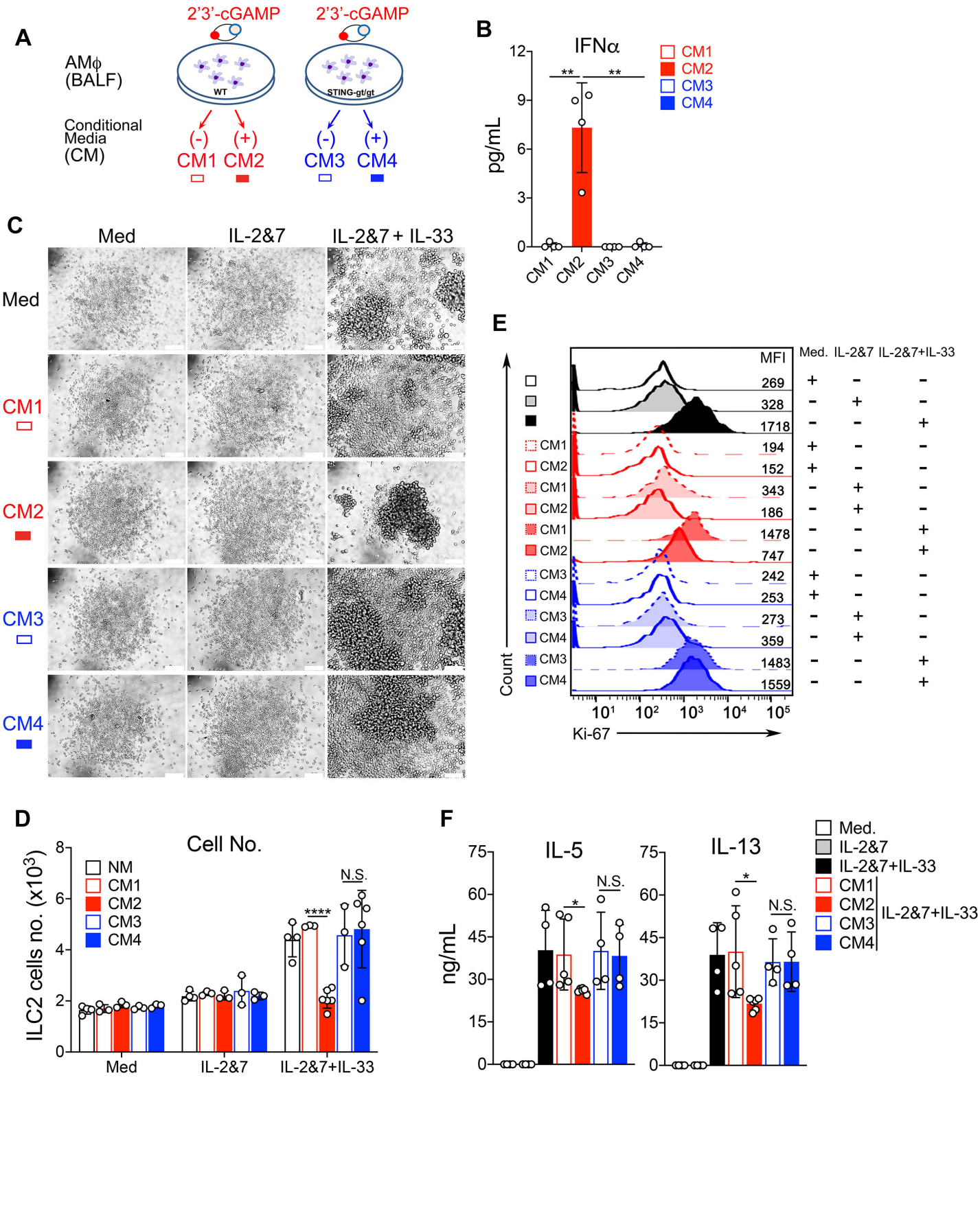
A
2'3'-cGAMP
2'3'-cGAMP
AMϕ (BALF)
WT
STING-gt/gt
Conditional Media (CM)
(-) (+)
CM1 CM2
(-) (+)
CM3 CM4
B
IFNα
CM1
CM2
CM3
CM4
pg/mL
**
**
C
Med
IL-2&7
IL-2&7 + IL-33
Med
CM1
CM2
CM3
CM4
D
Cell No.
NM
CM1
CM2
CM3
CM4
ILC2 cells no. (x10³)
****
N.S.
Med
IL-2&7
IL-2&7+IL-33
E
MFI
Med. IL-2&7 IL-2&7+IL-33
269
328
1718
194
152
343
186
1478
747
242
253
273
359
1483
1559
Count
Ki-67
F
IL-5
IL-13
ng/mL
*
N.S.
Med.
IL-2&7
IL-2&7+IL-33
CM1
CM2
CM3
CM4
IL-2&7+IL-33

Figure 8. 2'3'-cGAMP stimulates alveolar macrophages to produce ILC2-inhibitory factors. (**A**) The diagram showing the generation of conditional media from the ex vivo cultured AMΦ cells from WT or $STING^{gt/gt}$ mice that were stimulated with or without 2'3'-cGAMP. (**B**) The level of IFNα in the conditional media was measured by ELISA. (**C**) Light microscopic images showing the growth of mouse ILC2 cells in the presence of the corresponding conditional media as indicated. (**D**) FACS showing the number of murine ILC2 cells in the presence of the conditional media. (**E**) Ki-67 staining of mouse ILC2 cells in the presence of the conditional media. (**F**) ELISA measuring the production of IL-5 and IL-13 by mouse ILC2 cells in the presence of the conditional media. (Statistics for **D** was performed using Two-Way ANOVA, Turkey's multiple comparisons test by comparing mouse ILC2 treated with conditional media as indicated. P value ≥ 0.05 was not considered statistically significant [N.S.], * $p < 0.05$, **** $p < 0.0001$).

Figure 9

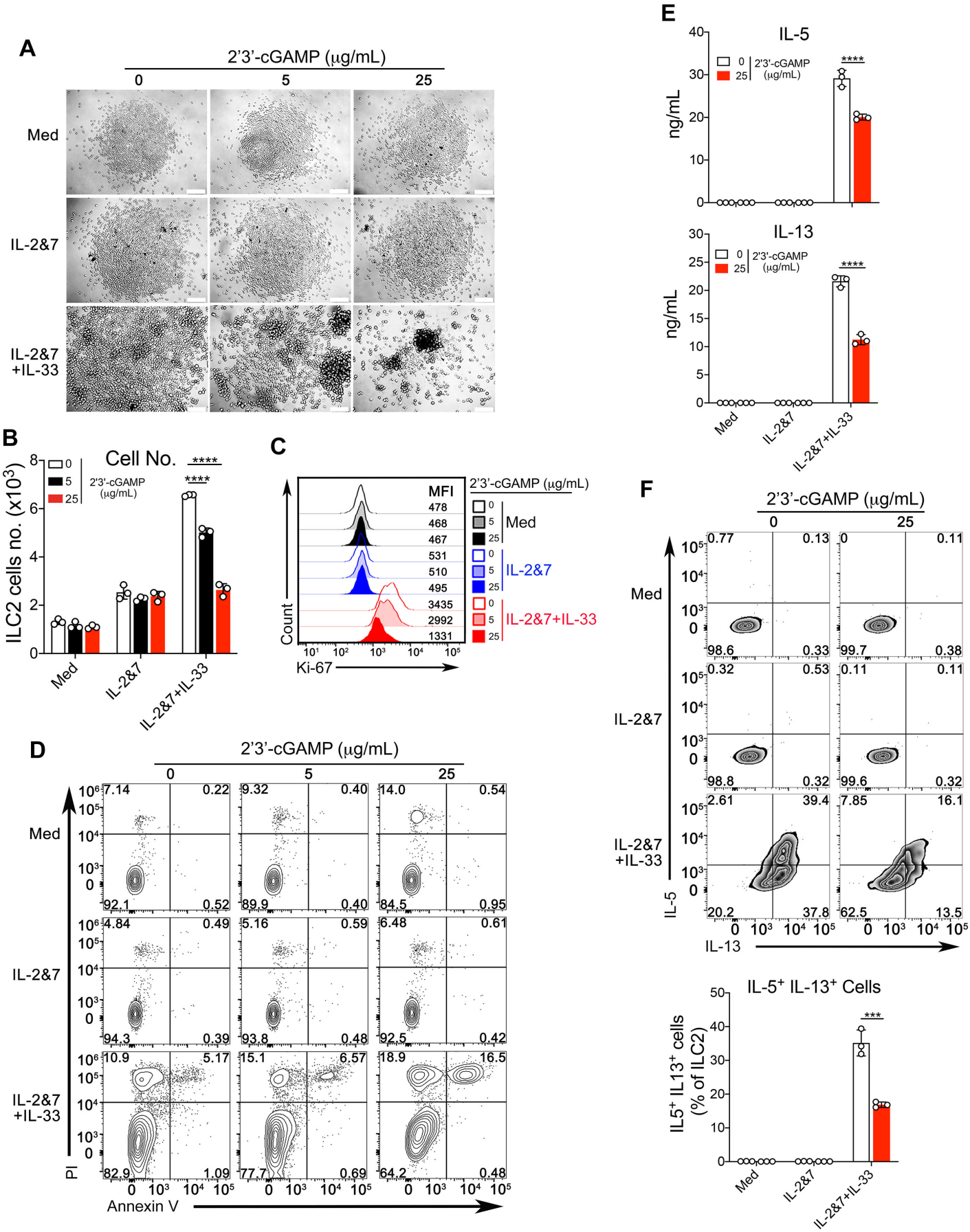
A
2'3'-cGAMP (μg/mL)
0
5
25
Med
IL-2&7
IL-2&7 +IL-33
B
Cell No.
****
****
0
5
25
2'3'-cGAMP (μg/mL)
ILC2 cells no. (x10³)
Med
IL-2&7
IL-2&7+IL-33
C
MFI
478
468
467
531
510
495
3435
2992
1331
2'3'-cGAMP (μg/mL)
Med
IL-2&7
IL-2&7+IL-33
Count
Ki-67
D
2'3'-cGAMP (μg/mL)
0
5
25
Med
IL-2&7
IL-2&7 +IL-33
PI
Annexin V
7.14
0.22
92.1
0.52
9.32
0.40
89.9
0.40
14.0
0.54
84.5
0.95
4.84
0.49
94.3
0.39
5.16
0.59
93.8
0.48
6.48
0.61
92.5
0.42
10.9
5.17
82.9
1.09
15.1
6.57
77.7
0.69
18.9
16.5
64.2
0.48
E
IL-5
0
25
2'3'-cGAMP (μg/mL)
****
ng/mL
IL-13
0
25
2'3'-cGAMP (μg/mL)
****
ng/mL
Med
IL-2&7
IL-2&7+IL-33
F
2'3'-cGAMP (μg/mL)
0
25
Med
IL-2&7
IL-2&7 +IL-33
IL-5
IL-13
0.77
0.13
98.6
0.33
0
0.11
99.7
0.38
0.32
0.53
98.8
0.32
0.11
0.11
99.6
0.32
2.61
39.4
20.2
37.8
7.85
16.1
62.5
13.5
IL-5⁺ IL-13⁺ Cells
***
IL5⁺ IL13⁺ cells (% of ILC2)
Med
IL-2&7
IL-2&7+IL-33

Figure 9. 2'3'-cGAMP directly suppresses the proliferation and cytokine production of mouse ILC2 cells. (**A**) Light microscopic images showing the growth of mouse ILC2 cells in the presence of the increased concentration of 2'3'-cGAMP. (**B**) FACS showing the number of murine ILC2 cells in the presence of the increased concentration of 2'3'-cGAMP. (**C**) Ki-67 staining of murine ILC2 cells in the presence of the increased concentration of 2'3'-cGAMP. (**D**) Cell death of mouse ILC2 cells in the presence of the increased concentration of 2'3'-cGAMP. (**E**) ELISA measuring the production of IL-5 and IL-13 by mouse ILC2 cells in the presence of the increased concentration of 2'3'-cGAMP. (**F**) Intracellular staining of IL-5 and IL-13 in mouse ILC2 cells treated with 2'3'-cGAMP (the percentage of the double-positive cells were quantified, lower). (Statistics was performed using Two-Way ANOVA, Turkey's multiple comparisons test by comparing media-treated mouse ILC2 to the individual treatment as indicated. P value ≥ 0.05 was not considered statistically significant, *** $p < 0.001$, **** $p < 0.0001$).

Figure 10

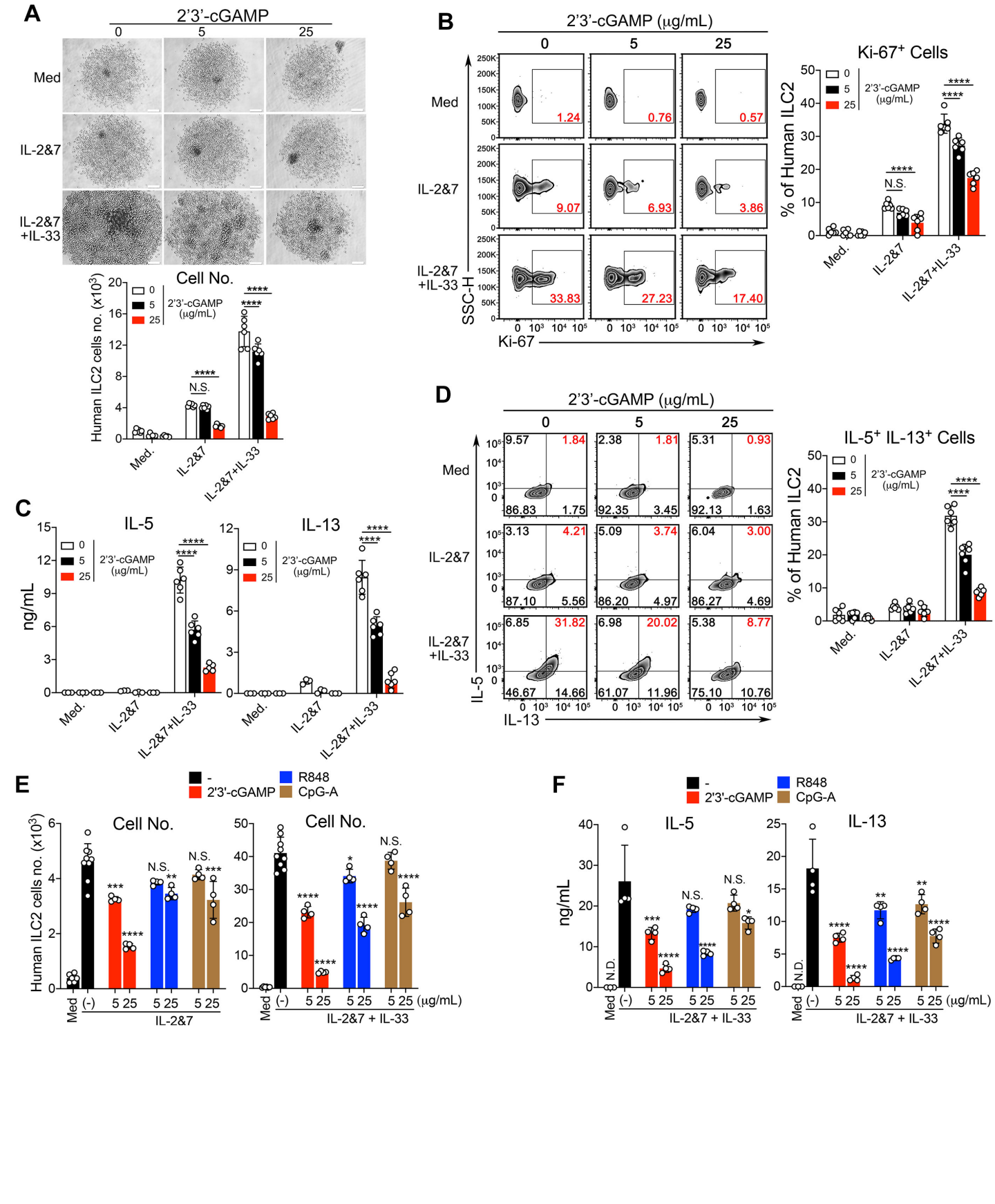
A
2'3'-cGAMP
0
5
25
Med
IL-2&7
IL-2&7 +IL-33
Cell No.
Human ILC2 cells no. (x10³)
2'3'-cGAMP (μg/mL)
N.S.
Med.
IL-2&7
IL-2&7+IL-33
B
2'3'-cGAMP (μg/mL)
1.24
0.76
0.57
9.07
6.93
3.86
33.83
27.23
17.40
SSC-H
Ki-67
Ki-67⁺ Cells
% of Human ILC2
C
IL-5
IL-13
ng/mL
D
9.57
1.84
2.38
1.81
5.31
0.93
86.83
1.75
92.35
3.45
92.13
1.63
3.13
4.21
5.09
3.74
6.04
3.00
87.10
5.56
86.20
4.97
86.27
4.69
6.85
31.82
6.98
20.02
5.38
8.77
46.67
14.66
61.07
11.96
75.10
10.76
IL-5
IL-13
IL-5⁺ IL-13⁺ Cells
E
-
2'3'-cGAMP
R848
CpG-A
Cell No.
Human ILC2 cells no. (x10³)
Med
(-)
5 25
IL-2&7
IL-2&7 + IL-33
(μg/mL)
N.S.
F
IL-5
IL-13
ng/mL
N.D.

Figure 10. 2'3'-cGAMP directly suppresses the proliferation and cytokine production of human ILC2 cells. (**A**) Light microscopic images and FACS showing the growth and number of human ILC2 cells in the presence of the increased concentration of 2'3'-cGAMP. (**B**) Ki-67 staining of human ILC2 cells in the presence of the increased concentration of 2'3'-cGAMP. (**C**) ELISA measuring the production of IL-5 and IL-13 by human ILC2 cells in the presence of the increased concentration of 2'3'-cGAMP. (**D**) Intracellular staining of IL-5 and IL-13 in human ILC2 cells treated with the increased concentration of 2'3'-cGAMP (the quantification of the percentage of the double-positive cells, right). (**E**) Human ILC2 cells cultured under either IL-2&7 or IL-2&7 + IL-33 were treated with 2'3'-cGAMP, R848 or CpG-A as indicated. FACS showing the growth of human ILC2 cells. (**F**) Same as (**E**). The production of IL-5 and IL-3 was measured by ELISA. The result is a representative of three independent experiments. (Statistics was performed using Two-Way ANOVA, Turkey's multiple comparisons test by comparing media or mock (-) -treated human ILC2 to the individual treatment as indicated. P value ≥ 0.05 was not considered statistically significant [N.S.], * $p < 0.05$, ** $p < 0.01$, *** $p < 0.001$, **** $p < 0.0001$).

Figure 11

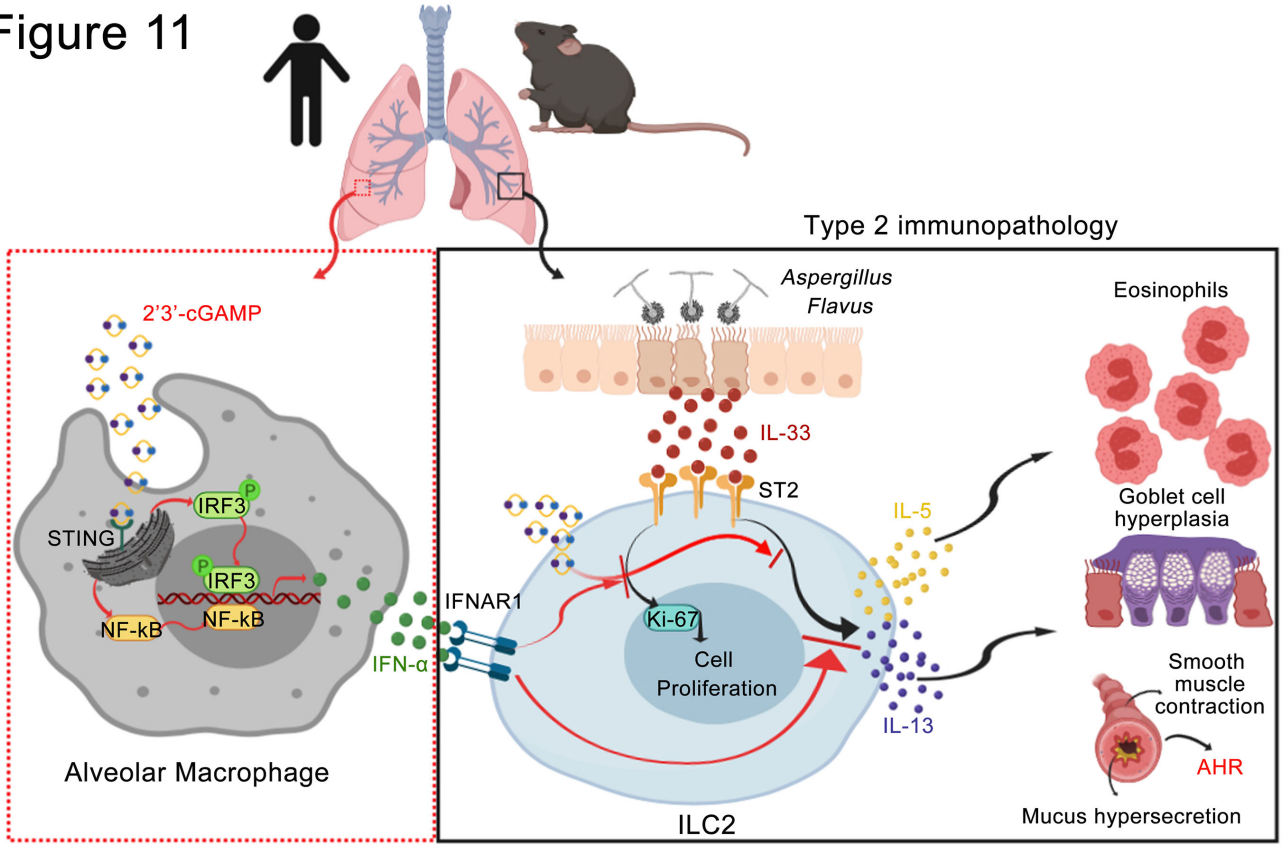

Figure 11. A proposed working model illustrates the potential mechanism through which 2'3'-cGAMP inhibits type 2 immunopathology by targeting human and mouse alveolar macrophages and ILC2 cells (Artwork was initially created in BioRender, https://app.biorender.com).